Knot theory and cluster varieties

Nicolas Pastant

UNIVERSITÉ DE STRASBOURG

ÉCOLE DOCTORALE MSII ED269

IRMA, UMR 7501

THÈSE présentée par :

Nicolas PASTANT

soutenue le : **20 décembre 2019**

pour obtenir le grade de : **Docteur de l'université de Strasbourg**

Discipline/ Spécialité : Mathématiques fondamentales

Théorie des nœuds et variétés amassées

THÈSE dirigée par :

M. FOCK Vladimir	Professeur, Université de Strasbourg

RAPPORTEURS :

M. TUMARKIN Pavel	Professeur, Durham University
M. ITENBERG Ilia	Professeur, Université Pierre et Marie Curie

---

AUTRES MEMBRES DU JURY :

M. BAUMANN Pierre	Chargé de recherches HDR, Université de Strasbourg
M. MASSUYEAU Gwénaël	Professeur, Université de Bourgogne

Théorie des nœuds et Variétés amassées

Nicolas Pastant

Institut de Recherche Mathématique Avancée
Université de Strasbourg
7 rue René Descartes
67084 Strasbourg Cedex

Thèse de doctorat sous la direction de

Vladimir Fock

Contents

Introduction

Le but de cette thèse est de donner de nouvelles applications de la théorie des variétés amassées à la théorie des nœuds, ou plus généralement à la topologie des variétés de dimension 3.

Motivés par l'étude de la positivité totale et des bases canoniques dans les groupes quantiques, Fomin et Zelevinsky [FZ02] ont introduit les algèbres amassées au début des années 2000. Les variétés amassées introduites par Fock et Goncharov [FG06a] sont des analogues géométriques des algèbres amassées. Elles apparaissent naturellement dans le contexte de la théorie de Teichmüller [FG07]. La combinatoire des algèbres et variétés amassées joue un rôle important dans de nombreux domaines. Nous citons en particulier : physique statistique [GK11] , théorie de Lie [FG06b], géométrie de Poisson [GSV03] et systèmes dynamiques discrets [KNS11].

La théorie des nœuds dont l'origine remonte aux travaux de Gauss sur l'indice d'entrelacement au 19^e sciècle est, elle aussi, liée à de nombreux domaines des mathématiques et de la physique. Les travaux de Jones [Jon85] ont notamment donné lieu au développement de la topologie quantique. Il est remarquable que, dans ce contexte, certains invariants de nœuds peuvent être exprimés comme fonction de partition de modèles issus de la mécanique statistique [Kau06]. De même, les groupes de tresses et certaines de leurs généralisations peuvent être interprétés du point de vue de la théorie de Lie [All02].

L'objectif de notre travail est de montrer que certains invariants de nœuds et tresses peuvent être exprimés comme des invariants de variétés amassées naturellement associés à des représentants diagrammatiques de ces objets topologiques.

Dans le premier chapitre nous rappelons, dans le paragraphe 1.1 les définitions des variétés amassées de Fock et Goncharov [FG06b] dans le cas particulier qui nous interesse, à savoir les variétés amassées de type $\mathcal{X}$ dans le cas simplement lacé et où le corps de base est $\mathbb{C}$. Dans ce cas ce sont des variétés complexes obtenues par recollement de tores algébriques $(\mathbb{C}^*)^n$ avec n fixé et où les applications de recollement sont des applications birationnelles appelées mutations dont la forme est définie de manière

précise à partir d'une matrice symétrique. Ces variétés sont munies d'une structure de Poisson. Nous présentons en particulier deux classes de variétés amassées dans le sens précédent.

- Les graphes bipartis plongés cellulairement dans une surface étudiés par Goncharov et Kenyon [GK11] que nous présentons dans le paragraphe 1.2.2
- Les variétés amassées construites à partir d'un diagramme de Dynkin par Fock et Goncharov [FG06b] présentées dans le paragraphe 1.3

Dans les paragraphes correspondants, nous rappelons la construction des invariants de ces variétés, la fonction de partition de dimères dans le premier cas et l'application d'évaluation dans le second. Dans le cas particulier des diagrammes des séries A et $\hat{A}$, la seconde classe de variétés amassées est décrite par Fock est Marshakov [FM14] à l'aide de diagrammes introduits par Thurston [Thu04]. Cette description est rappelée dans le paragraphe 1.4 dans le cas de la série A et dans le paragraphe 1.5 pour la série $\hat{A}$.

Dans le second chapitre nous donnons les définitions des objets de la théorie des nœuds que nous étudions ainsi que leurs invariants que nous réinterprétons du point de vue des variétés amassées, à savoir, dans le paragraphe 2.2, la torsion de Milnor-Turaev de l'extérieur des entrelacs et deux méthodes de calcul de cette dernière : la méthode des τ-chaînes de Turaev [Tur86] et la méthode des contractions de chaînes. Nous rappelons dans le paragraphe 2.4 les définitions des groupoïdes des tresses colorées orientées dans les cas planaires et cylindriques ainsi que les représentations de Burau réduites et non réduites de ces groupoïdes [Bur35] [SW01] [GTW17].

Le chapitre 3 constitue le cœur de cette thèse dans lequel nous présentons et démontrons nos résultats :

- Nous étendons et interprétons géométriquement le modèle de dimères pour le polynôme d'Alexander de Cohen, Dasbach et Russel [CDR14]. À partir d'un diagramme d'entrelacs nous construisons dans le paragraphe 3.1.3 un graphe biparti qui encode une structure cellulaire sur l'extérieur de l'entrelacs relativement à son bord. Nous décrivons dans le paragraphe 3.1.4 une pondération de ce graphe qui encode un système de coefficients locaux induit par le morphisme d'abélianisation du groupe fondamental de l'entrelacs. Cette donnée nous permet de décrire dans le paragraphe 3.1.5 la torsion de Milnor de l'extérieur d'un entrelacs comme une fonction de partition de dimères.
- Dans le paragraphe 3.2 nous associons aux tresses colorées orientées classiques des sous-variétés des variétés amassées construites à partir du digramme de Dynkin de type A. En composant avec l'application d'évaluation nous obtenons une

représentation du groupoïde des tresses colorées orientées classiques. Pour la représentation standard de $PGL_n(\mathbb{C})$ nous obtenons les matrices de la représentation de Burau réduite pour une version de notre construction, et celle de la représentation de Burau non réduite pour une version en un certain sens duale.

- Nous décrivons dans le paragraphe 3.3 une construction similaire au point précédent pour le groupoïde des tresses colorées orientées cylindriques. Les variétés amassées impliquées sont dans ce cas, celles construites à partir des diagrammes de Dynkin de type $\hat{A}$.

On peut résumer nos résultats dans le tableau suivant :

Objet noué	Variétés amassées associées	Invariant amassé correspondant	Invariant de l'objet noué
Entrelacs dans $\mathbb{S}^3$	Graphe biparti plongé	Fonction de partition de dimères	Torsion de Milnor de l'extérieur de l'entrelacs
Tresse colorée orientée	Variétés associées à $PGL_n(\mathbb{C})$	Application d'évaluation	Représentations généralisées de Burau (réduites et non réduites)
Tresse cylindrique colorée orientée	Variétés associées à $\widehat{PGL}_n^{\#}(\mathbb{C})$	Application d'évaluation	Représentation de Burau généralisée

Chapter 1

Cluster varieties

In this chapter we present the definition of the cluster $\mathcal{X}$-varieties in the particular case that we need for our constructions. More precisely we describe the cluster $\mathcal{X}$-varieties introduced by V. Fock and A. Goncharov following their paper [FG06b] but restricting to the skew-symmetric case with complex numbers as base field. If we restrict ourselves to $\mathbb{C}$, the cluster $\mathcal{X}$-varieties have a structure of a complex manifold.

We then describe two objects closely related to cluster varieties, namely Thurston diagrams and embedded bipartite graphs.

Finally, we describe the cluster varieties associated to split semi-simple Lie groups with trivial center, again following [FG06b] and again, in the simply laced and complex case.

1.1 Cluster $\mathcal{X}$-manifolds

1.1.1 Definitions

A cluster seed $\mathbf{I}$ is a triple (I, I_0, ε) where I is a finite set, I_0 is a subset of I and ε is a skew-symmetric matrix ε_{ij}, where $\varepsilon_{ij} \in \mathbb{Z}$ unless $(i, j) \in I_0 \times I_0$.

The elements of I are called vertices and those of I_0 frozen vertices.

To a seed $\mathbf{I}$ is associated a torus $\mathcal{X}_{\mathbf{I}} = (\mathbb{C}^*)^I$ with a Poisson structure given by

$$\{x_i, x_j\} = \varepsilon_{ij} x_i x_j$$

where $\{x_i \mid i \in I\}$ are the standard coordinates.

Let $\mathbf{I} = (I, I_0, \varepsilon)$ and $\mathbf{I'} = (I', I'_0, \varepsilon')$ be two seeds and $k \in I$. A mutation in the vertex k is an isomorphism $\mu_k : I \to I'$ satisfying the following conditions :

1. $\mu_k(I_0) = I'_0$
2. $\varepsilon'_{\mu_k(i)\mu_k(j)} = \begin{cases} -\varepsilon_{ij} & \text{if } i = k \text{ or } j = k \\ \varepsilon_{ij} + \varepsilon_{ik}\max(0, \varepsilon_{kj}) & \text{if } \varepsilon_{ik} \geq 0 \\ \varepsilon_{ij} + \varepsilon_{ik}\max(0, -\varepsilon_{kj}) & \text{if } \varepsilon_{ik} < 0 \end{cases}$

A symmetry of a seed $\mathbf{I} = (I, I_0, \varepsilon)$ is an automorphism σ of the set I such that $\sigma(I_0) = I_0$ and $\varepsilon_{\sigma(i)\sigma(j)} = \varepsilon_{ij}$.

Symmetries and mutations induce (rational) maps between the corresponding seed $\mathcal{X}$-tori which are denoted by the same symbols μ_k and σ and given by the formulae

$$x_{\sigma(i)} = x_i$$

and

$$x_{\mu_k(i)} = \begin{cases} x^{-1} & \text{if } i = k \\ x_i(1 + x_k)^{\varepsilon_{ik}} & \text{if } \varepsilon_{ik} \geq 0 \text{ and } i \neq k \\ x_i(1 + (x_k)^{-1})^{\varepsilon_{ik}} & \text{if } \varepsilon_{ik} \leq 0 \text{ and } i \neq k \end{cases}$$

A cluster transformation between two seeds and between two seed $\mathcal{X}$-tori is a composition of symmetries and mutations. Two seeds are called equivalent if they are related by a cluster transformation. The equivalence class of a seed $\mathbf{I}$ is denoted by $|\mathbf{I}|$. A cluster $\mathcal{X}$-variety is obtained by taking a union of all seed $\mathcal{X}$-tori related to a given seed $\mathbf{I}$ by cluster transformation and gluing them together using the above birational isomorphisms. It is denoted by $\mathcal{X}_{|\mathbf{I}|}$.

Cluster transformations preserve the Poisson structure. In particular a cluster $\mathcal{X}$-manifold has a canonical Poisson structure.

1.1.2 Amalgamation

Let $\mathbf{I} = (I, I_0, \varepsilon)$ and $\mathbf{J} = (J, J_0, \eta)$ be two seeds and let L be a set embedded into both I_0 and J_0. The amalgamation of $\mathbf{I}$ and $\mathbf{J}$ is a seed $\mathbf{K} = (K, K_0, \zeta)$ such that $K = I \cup_L J$, $K_0 = I_0 \cup_L J_0$ and

$$\zeta_{ij} = \begin{cases} 0 & \text{if } i \in I - L \text{ and } j \in J - L \\ 0 & \text{if } i \in J - L \text{ and } j \in I - L \\ \eta_{ij} & \text{if } i \in I - L \text{ or } j \in I - L \\ \varepsilon_{ij} & \text{if } i \in J - L \text{ or } j \in J - L \\ \varepsilon_{ij} + \eta_{ij} & \text{if } i, j \in L \end{cases}$$

This operation induces a homomorphism $\mathcal{X}_{\mathbf{I}} \times \mathcal{X}_{\mathbf{J}} \to \mathcal{X}_{\mathbf{K}}$ between the corresponding seed $\mathcal{X}$-tori given by the rule

$$z_i = \begin{cases} x_i & \text{if } i \in I - L \\ y_i & \text{if } i \in J - L \\ x_i y_i & \text{if } i \in L \end{cases}$$

The induced homomorphism respects the Poisson structure and commutes with cluster transformations, thus is defined for the cluster $\mathcal{X}$-manifolds.

If there is a subset $L' \subset L$ such that $\varepsilon_{ij} + \eta_{ij} \in \mathbb{Z}$ when $i, j \in L$ then we can defrost the vertices of L' getting a new seed $(K, K_0 - L', \zeta)$ where we can mutate the elements of L' as well.

1.2 Thurston diagrams and embedded bipartite graphs

1.2.1 Thurston diagrams

Thurston diagrams are a special type of diagrams drawn on a surface, introduced by Dylan Thurston in the paper [Thu04]. As observed by Thurston and Henriques in [Thu04], Thurston diagrams can be interpreted as a cluster seed. Every Thurston diagram defines a cluster seed (a chart of a cluster manifold).

A Thurston diagram on an oriented surface Σ is an isotopy class of collections of oriented curves, such that all intersection points are triple and the orientation of the curves at every intersection point is alternating. The curves may either be closed or go from boundary to boundary. An example of a Thurston diagram in a disc is shown in Figure1.1.

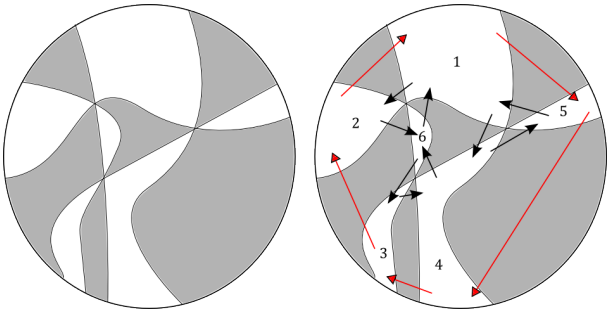

Figure 1.1: Thurston diagram on a disc and exchange relations.

The orientation condition at the intersection points implies that the segments of the curves bounding a face are oriented either clockwise (in this case the face is called white) or counter-clockwise (in this case the face is called gray). All neighboring faces of a white face are gray and vice versa. In the figure we did not indicate the orientation of the curves since it can be restored from the color of the faces. Thurston diagrams admit four kinds of modifications shown in Figure1.2.

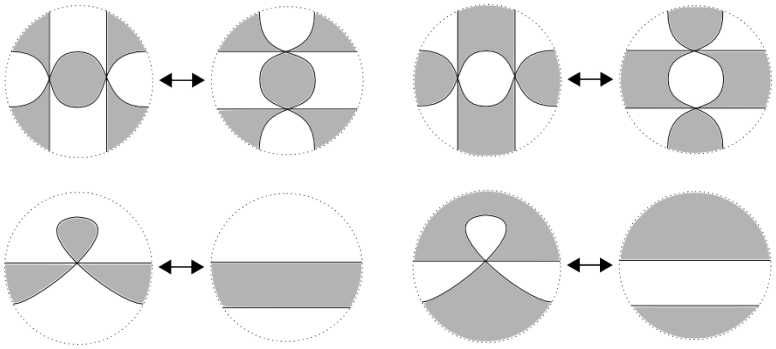

Figure 1.2: Thurston moves and reductions.

The first two, called Thurston moves, do not change the number of faces. The two

others reduce the number of faces and are called Thurston reductions. A move can be performed each time we have a monogon or a bigon. Diagrams where we cannot apply a Thurston reduction are called minimals.

Thurston diagrams and cluster varieties

We can define a cluster variety starting from an equivalence class of Thurston diagrams. The charts of this manifold correspond to particular diagrams in a given class and Thurston moves correspond to mutations. Cluster variables parameterizing a chart are assigned to white faces. Faces neighboring the boundary correspond to frozen variables.

The exchange matrix ε_{ij} is defined as follows (see Figure 2): Draw three arrows connecting white faces around every triple intersection and directed counter-clockwise. And connect every pair of white faces partially bounded by the boundary of the surface by a **gray** arrow, pointing to the right if viewed from inside the surface.

The value of ε_{ij} is equal to the number of arrows from the white face i to the white face j minus the numbers of arrows in the inverse direction. The gray arrows are counted with a $1/2$ coefficient.

There is a notion of duality for Thurston diagrams. If we reverse the orientation of all curves, or equivalently, if we exchange white and grey faces we obtain a new diagram. The relation between the associated cluster varieties is not clear but, as it will be seen in Chapter 3, given a braid representative, the cluster manifold corresponding to the Burau representation and the cluster manifold corresponding to the reduced Burau representation are related, from the Thurston diagrams point of view, by this notion of duality.

1.2.2 Bipartite graphs

We describe, following the paper of A. Goncharov and R. Kenyon [GK11] the relation between embedded bipartite graphs and cluster varieties.

Let Γ be a graph, denote by E_Γ and V_Γ the set of its edges and vertices, respectively. A dimer configuration on Γ is a subset $D \subset E_\Gamma$, such that every vertex is contained in exactly one edge of D. Denote by $\mathcal{D}_\Gamma$ the set of all dimer configurations on Γ, which we assume to be nonempty. Fix a function $\mathbf{A} : e \mapsto A_e$ associating a complex number, called weight, to any edge $e \in E_\Gamma$.

Consider the sum over all dimer configurations

$$S_\Gamma(\mathbf{A}) = \sum_{D \in \mathcal{D}_\Gamma} \prod_{e \in D} A_e$$

and call it the dimer partition function of the graph Γ. This partition function is a polynomial of the weight variables A_e with unit coefficients.

Let Γ be a surface graph, that is, a graph embedded in a compact surface Σ in such a way that the connected components of $\Sigma - \Gamma$, that we will call faces, are contractible. It is homotopy equivalent to an open surface $\Sigma_0 \subset \Sigma$ obtained by adding a puncture in every face. A bipartite graph is a graph with vertices of two types, black and white, such that each has one black and one white vertex.

A line bundle on a graph Γ is given by assigning a 1-dimensional complex vector space V_v to each vertex v of Γ. A connection on V is a choice of isomorphism $\phi_{vv'} : V_v \to V_{v'}$ whenever v and v' are adjacent, satisfying $\phi_{v'v} = \phi_{vv'}^{-1}$. Let $\mathcal{L}_\Gamma$ be the moduli space of line bundles with connections on a graph Γ. Any oriented loop L gives rise to a function W_L on $\mathcal{L}_\Gamma$ given by the monodromy of a line bundle with connection along L. We have $W_{-L} = W_L^{-1}$, where $-L$ is the loop L with the opposite orientation.

Kasteleyn weighting

A Kasteleyn line bundle with connection on a bipartite surface graph is a line bundle with connection with monodromy $(-1)^{l/2+1}$ around faces having l edges, and ± 1 around topologically nontrivial loops.

1.2.3 Relation between Thurston diagrams and bipartite graphs

In order to construct a bipartite graph out of a Thurston diagram we put a black vertex at every triple point and a white vertex in every gray face. Then we draw three edges from each black vertex inside the three gray sectors, meeting at this vertex, to the respective white vertices.

1.3 Cluster $\mathcal{X}$-manifolds constructed from a Dynkin diagram

In their paper [FG06b] Fock and Goncharov associate to a Dynkin diagram a family of cluster $\mathcal{X}$-varieties and a map from these varieties to the corresponding centerless semi-simple Lie group. We present here their construction in the simply laced case.

Let Π be the set of positive simple roots and Π^- the set of negative simple roots. We denote by $C_{\alpha\beta} = 2\frac{(\alpha,\beta)}{(\alpha,\alpha)}$ $\alpha, \beta \in \Pi$ the Cartan matrix. Let $\mathfrak{W}$ be the semigroup freely generated by the positive and negative simple roots. Let $\alpha \in \Pi$ be a simple root, we denote its opposite in Π^- by $\bar{\alpha}$.

We consider the braid semigroup $\mathfrak{B}$ which is defined to be the quotient of $\mathfrak{W}$ by the following relations

$$\alpha\bar{\beta} = \bar{\beta}\alpha$$
$$\alpha\beta\alpha = \beta\alpha\beta \text{ and } \bar{\alpha}\bar{\beta}\bar{\alpha} = \bar{\beta}\bar{\alpha}\bar{\beta} \qquad \text{if } C_{\alpha\beta} = C_{\beta\alpha} = -1$$

We denote by $p : \mathfrak{W} \to \mathfrak{B}$ the canonical projection. We also introduce the Hecke semigroup $\mathfrak{H}$ which is the further quotient of $\mathfrak{B}$ by the relations

$$\alpha^2 = \alpha \; ; \; \bar{\alpha}^2 = \bar{\alpha}$$

An element of $\mathfrak{W}$ or $\mathfrak{B}$ is said to be reduced if it is of minimal length among the elements having the same image in $\mathfrak{H}$.

1.3.1 Cluster $\mathcal{X}$-varieties related to the braid semigroup

To every word in the braid semigroup is associated a cluster variety. To each representative corresponds a chart of the variety. The charts are related by cluster transformations.

To an element $B \in \mathfrak{B}$ is associated a cluster manifold. Given an element $D \in \mathfrak{W}$, a seed $\mathbf{J}(D) = (J(D), J_0(D), \varepsilon(D))$ is defined.

Let α be a positive simple root, we consider new elements α' and α'' The seed $\mathbf{J}(\alpha)$ is defined by

$$J(\alpha) = J_0(\alpha) := (\Pi - \{\alpha\}) \cup \{\alpha'\} \cup \{\alpha''\}$$

There is a decoration map

$$\pi : J(\alpha) \to \Pi$$

which sends α' and α'' to α and is the identity map on $\Pi - \alpha$.

The matrix $\varepsilon(\alpha)$ is defined as follows : its entry $\varepsilon(\alpha)_{\beta\gamma}$ is zero unless one of the indices is decorated by α. Further

$$\varepsilon(\alpha)_{\alpha'\beta} = \frac{C_{\alpha\beta}}{2}, \quad \varepsilon(\alpha)_{\alpha''\beta} = -\frac{C_{\alpha\beta}}{2}, \quad \varepsilon(\alpha)_{\alpha'\alpha''} = -1$$

In the case where D is a negative simple root $\bar{\alpha}$ we have

$$J(\bar{\alpha}) = J_0(\bar{\alpha}) := (\Pi^- - \{\bar{\alpha}\}) \cup \{\bar{\alpha}'\} \cup \{\bar{\alpha}''\}$$

and a similar decoration $\pi : J(\bar{\alpha}) \to \Pi$ The antisymmetric matrix is obtained by reversing the signs, using the obvious identification of $J(\bar{\alpha})$ and $J(\alpha)$, that is we set $\varepsilon(\bar{\alpha}) := -\varepsilon(\alpha)$

$$\varepsilon(\bar{\alpha})_{\alpha'\beta} = -\frac{C_{\alpha\beta}}{2}, \quad \varepsilon(\bar{\alpha})_{\alpha''\beta} = \frac{C_{\alpha\beta}}{2}, \quad \varepsilon(\bar{\alpha})_{\alpha'\alpha''} = 1$$

Let us describe the general case. First, observe that the subset of the elements decorated by a simple root has one element unless this root is α, where there are two elements. There is a natural linear order on the subset of elements of $\mathbf{J}(\alpha)$ decorated by a given simple positive root γ, it is given by (α', α'') in the only nontrivial case when $\alpha = \gamma$. So for a given simple positive root γ, there are the minimal and the maximal elements decorated by γ.

Définition Let $D = \alpha_1 ... \alpha_n \in \mathfrak{W}$, then $J(D)$ is obtained by gluing the sets $J(\alpha_1), ..., J(\alpha_n)$ as follows. For every $\gamma \in \Pi$, and for every $i = 1, ..., n-1$, we glue the maximal γ- decorated element of $J(\alpha_i)$ and the minimal γ-decorated element of $J(\alpha_{i+1})$.

The seed $\tilde{\mathbf{J}}(D)$ is the amalgamated product for this gluing data of the seeds $\mathbf{J}(\alpha_1), ..., \mathbf{J}(\alpha_n)$.

The seed $\tilde{\mathbf{J}}(D)$ has only frozen vertices, that is $\tilde{J}(D) = \tilde{J}_0(D)$. To define the seed $\mathbf{J}(D)$ we will defrost some of them. In definition 1.3.1 we glue only elements decorated by the same positive simple root. Thus the obtained set $J(D)$ has a natural decoration $\pi : J(D) \to \Pi$ extending those of the subsets $J(\alpha_i)$. Moreover, for every $\gamma \in \Pi$ the subset of γ-decorated elements of $J(D)$ has a natural linear order induced by the ones on $J(\alpha_i)$ and the linear order of the word D.

Définition The subset $J_0(D)$ is the union over $\gamma \in \Pi$ of the extremal (i.e minimal and maximal) elements for the defined above linear order on the γ-decorated part of $J(D)$.

The seed $\mathbf{J}$ is obtained from the seed $\tilde{\mathbf{J}}$ by reducing $\tilde{J}_0(D)$ to the subset $J_0(D)$.

Observe that $\varepsilon_{\alpha\beta}$ is integral unless both α and β are in $J_0(D)$. Thus the integrality condition for $\varepsilon_{\alpha\beta}$ holds.

We also give the alternative definition of the sets $J(D)$ and $J_0(D)$. Given a simple root $\alpha \in \Pi$, denote by $n^\alpha(D)$ the number of occurrences of α and $\bar{\alpha}$ in the word D. We set

$$J^\alpha(D) := \{(\alpha, i) | \alpha \in \Pi, 0 \leq i \leq n^\alpha\}, \quad J_0^\alpha(D) := \{(\alpha, 0)\} \cup \{(\alpha, n^\alpha)\}$$

Then $J(D)$ (resp ${}^J_0(D)$) is the disjoint union of $J^\alpha(D)$ (resp $J_0^\alpha(D)$) for all $\alpha \in \Pi$. Observe that if a root α does not enter the word D then $J_0^\alpha(D) = J^\alpha(D)$ is a one element set.

We can picture elements of the set $J(D)$ as associated to the intervals between walls made by $\alpha, \bar{\alpha}$ or the ends of the word D for some root α. If at least one wall is just the end of D, the corresponding element of $J(D)$ belongs to $J_0(D)$.

1.3.2 Cluster $\mathcal{X}$-varieties related to the Hecke semigroup

Let $\pi : \mathfrak{B} \to \mathfrak{H}$ be the canonical projection from the braid semigroup to the Hecke semigroup. Considered as a projection of sets it has a canonical splitting $s : \mathfrak{H} \to \mathfrak{B}$. Namely, for every $H \in \mathfrak{H}$ there is a unique reduced element $s(H)$ in $\pi^{-1}(H)$, the reduced representative of H in $\mathfrak{B}$. So, given an element $H \in \mathfrak{H}$, there is a cluster variety $\mathcal{X}_{s(H)}$.

A rational map of cluster $\mathcal{X}$-manifolds is a cluster projection if, in a certain cluster parametrization system, it is obtained by forgetting one or more cluster coordinates.

If $H \in \mathfrak{H}$, the map $ev : \mathcal{X}_H \hookrightarrow G$ is injective. In the non-affine case there is an element of maximal length in $\mathfrak{H}$ and the corresponding cluster manifold provides G with cluster coordinates.

1.3.3 The evaluation map

We describe the evaluation map from the cluster $\mathcal{X}$-manifolds related to the braid semigroup of a Dynkin diagram, to the adjoint group G of the corresponding complex semisimple Lie group.

Recall the torus $\mathcal{X}_{\mathbf{J}(D)} = (\mathbb{C}^*)^{J(D)}$ and the natural coordinates $\{x_i^\alpha\}$ on it. Let us define the map

$$ev : \mathcal{X}_{\mathbf{J}(D)} \to G$$

In order to do so we are going to construct a sequence of group elements, each of which is either a constant or depends on just one coordinate of $\mathcal{X}_{\mathbf{J}(D)}$. The product of the elements of the sequence will give the desired map.

Let $f_\alpha, h_\alpha, e_\alpha$ be Chevalley generators of the Lie algebra $\mathfrak{g}$ of G. They are defined up to an action of the Cartan subgroup H of G. Let $\{h^\alpha\}$ be another basis of the Cartan subalgebra defined by the property :

$$[h^\alpha, e_\beta] = \delta^\alpha_\beta e_\beta, \quad [h^\alpha, f_\beta] = -\delta^\alpha_\beta f_\beta$$

This basis is related to the basis $\{h^\alpha\}$ via the Cartan matrix $\sum_\beta C_{\alpha\beta} h^\beta = h_\alpha$. The elements h_α and h^α give rise to cocharacters H_α and H^α called the coroot and the coweight corresponding to the simple root α.

Since the evaluation map is constructed with the coweights the image of the evaluation map is contained in the centerless form of the group associated to the Dynkin diagram.

We have $H_\alpha(x) = \exp(\log(x) h^\alpha)$. Let us introduce the group elements $\mathbf{E}^\alpha = \exp e_\alpha$ and $\mathbf{F}^\alpha = \exp f_\alpha$.

Replace the letters in D by the group elements using the rule $\alpha \to \mathbf{E}^\alpha, \bar{\alpha} \to \mathbf{F}^\alpha$. For $\alpha \in \Pi$ and for any $(\alpha, i) \in J(D)$ insert $H^\alpha(x_i^\alpha)$ between the corresponding walls. The choice in placing every H is unessential since it commutes with all E's and F's unless they are marked by the same root. In other words the sequence of group elements is defined by the following requirements :

- The sequence of **E**'s and **F**'s reproduce the sequence of the letters in the word D.
- Any H depends on its own variable x_i^α.
- There is at least one $\mathbf{E}^\alpha$ or $\mathbf{F}^\alpha$ between any two H^α's.
- The number of H^α's is equal to the total number of $\mathbf{E}^\alpha$'s and $\mathbf{F}^\alpha$'s plus one.

1.3.4 Properties of the spaces $\mathcal{X}_B$

Theorem 1.1 *[FG06b] Let A, B be arbitrary words and $\alpha, \beta \in \Pi$. There are the following rational maps commuting with the map ev :*

1. $\mathcal{X}_{\mathbf{J}(A\bar{\alpha}\beta B)} \to \mathcal{X}_{\mathbf{J}(A\beta\bar{\alpha}B)}$ *if* $\alpha \neq \beta$.
2. $\mathcal{X}_{\mathbf{J}(A\alpha\beta B)} \to \mathcal{X}_{\mathbf{J}(A\beta\alpha B)}$ *and* $\mathcal{X}_{\mathbf{J}(A\bar{\alpha}\bar{\beta}B)} \to \mathcal{X}_{\mathbf{J}(A\bar{\beta}\bar{\alpha}B)}$ *if* $C_{\alpha\beta} = 0$.
3. $\mathcal{X}_{\mathbf{J}(A\alpha\beta\alpha B)} \to \mathcal{X}_{\mathbf{J}(A\beta\alpha\beta B)}$ *and* $\mathcal{X}_{\mathbf{J}(A\bar{\alpha}\bar{\beta}\bar{\alpha}B)} \to \mathcal{X}_{\mathbf{J}(A\bar{\beta}\bar{\alpha}\bar{\beta}B)}$ *if* $C_{\alpha\beta} = C_{\beta\alpha} = -1$.
4. $\mathcal{X}_{\mathbf{J}(A\alpha\alpha B)} \to \mathcal{X}_{\mathbf{J}(A\alpha B)}$ *and* $\mathcal{X}_{\mathbf{J}(A\bar{\alpha}\bar{\alpha}B)} \to \mathcal{X}_{\mathbf{J}(A\bar{\alpha}B)}$.
5. $\mathcal{X}_{\mathbf{J}(A)} \times \mathcal{X}_{\mathbf{J}(B)} \to \mathcal{X}_{\mathbf{J}(AB)}$.

Maps 1 and 2 are isomorphisms, map 3 is a cluster transformation. Map 4 is a composition of a cluster transformation and a projection along the coordinate axis. Map 5 is an amalgamated product. Map ev is a Poisson map. The maps 1 to 5 are also Poisson maps.

Remark – It is not true that a mutation of a cluster seed $\mathbf{J}(D)$ is always a cluster seed corresponding to another word of the semigroup.

Relations between the generators

There are the following identities between the generators $\mathbf{E}^\alpha, H^\alpha(x), \mathbf{F}^\alpha$:

$$\begin{aligned}
\mathbf{E}^\alpha H^\alpha(x)\mathbf{E}^\alpha &= H^\alpha(1+x)\mathbf{E}^\alpha H^\alpha(1+x^{-1})^{-1} \\
\mathbf{E}^\alpha\mathbf{E}^\beta &= \mathbf{E}^\beta\mathbf{E}^\alpha \text{if } C_{\alpha\beta} = 0 \\
\mathbf{E}^\alpha H^\alpha(x)\mathbf{E}^\beta\mathbf{E}^\alpha &= H^\alpha(1+x)H^\beta(1+x^{-1})^{-1}\mathbf{E}^\beta H^\beta(x^{-1})\mathbf{E}^\alpha\mathbf{E}^\beta H^\alpha(1+x^{-1})^{-1}H^\beta(1+x) \text{if } C_{\alpha\beta} = -1 \\
\mathbf{F}^\alpha H^\alpha(x)\mathbf{E}^\alpha &= \left(\prod_{\beta\neq\alpha} H^\beta(1+x)^{-C_{\alpha\beta}}\right) H^\alpha(1+x^{-1})^{-1}\mathbf{E}^\alpha H^\alpha(x^{-1})\mathbf{F}^\alpha H^\alpha(1+x^{-1})^{-1} \\
\mathbf{F}^\alpha\mathbf{E}^\beta &= \mathbf{E}^\beta\mathbf{F}^\alpha \text{if } \alpha \neq \beta
\end{aligned}$$

There is another relation especially important in our context.

$$\mathbf{E}^\alpha H^\alpha(-1)\mathbf{E}^\alpha = H^\alpha(-1)$$

Applying the antiautomorphism of $\mathfrak{g}$ which acts as the identity on the Cartan subalgebra and interchanges $\mathbf{F}^\alpha$ and $\mathbf{E}^\alpha$, we obtain similar formulas for $\bar{\alpha}\bar{\alpha} \to \bar{\alpha}, \bar{\alpha}\bar{\beta} \to \bar{\beta}\bar{\alpha}$ and $\bar{\alpha}\bar{\beta}\bar{\alpha} \to \bar{\beta}\bar{\alpha}\bar{\beta}$. For example if $C_{\alpha\beta} = C_{\beta\alpha} = -1$, then

$$\mathbf{F}^\alpha H^\alpha(x)\mathbf{F}^\beta\mathbf{F}^\alpha = H^\alpha(1+x^{-1})^{-1}H^\beta(1+x)\mathbf{F}^\beta H^\beta(x^{-1})\mathbf{F}^\alpha\mathbf{F}^\beta H^\alpha(1+x)H^\beta(1+x^{-1})^{-1}$$

1.4 A_n Cluster $\mathcal{X}$-manifolds

In this section we describe the cluster $\mathcal{X}$-manifolds associated to a Dynkin diagram in the special case of the A type.

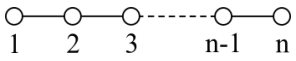

Figure 1.3: Dynkin diagram of type A_n.

Let us consider the A_n type Dynkin diagram. We label its nodes from left to right with integers from 1 to n. See Figure 1.3

The Weyl group is generated by the positive simple roots s_i where i is the corresponding labeling of the node; and subject to the following relations

$$\begin{aligned} s_i s_{i+1} s_i &= s_{i+1} s_i s_{i+1} && \text{for } i = 1, ..., n \\ s_i s_j &= s_j s_i && \text{for distant } i, j = 1, ..., n \\ s_i^2 &= 1 && \text{for } i = 1, ..., n \end{aligned}$$

The Weyl group associated to the Dynkin diagram A_n is isomorphic to the symmetric group on $n+1$ letters S_{n+1}. We denote the group elements corresponding to s_i by E_i, F_i and H_i. In the standard representation they have the following form

$$H_i(x) = \begin{pmatrix} x & 0 & & \cdots & & 0 \\ 0 & \ddots & & & & \\ & & x & & & \vdots \\ \vdots & & & 1 & & \\ & & & & \ddots & 0 \\ 0 & & \cdots & & 0 & 1 \end{pmatrix} \qquad E_i = F_i^T = \begin{pmatrix} 1 & 0 & & \cdots & & 0 \\ 0 & \ddots & & & & \\ & & 1 & 1 & & \vdots \\ \vdots & & & 1 & & \\ & & & & \ddots & 0 \\ 0 & & \cdots & & 0 & 1 \end{pmatrix}$$

where the last line of $H_i(x)$ with an x entry is the i-th line and the off-diagonal element of E_i is the in the i-th line.

1.4.1 Thurston diagrams and cluster varieties associated to $PGL_n(\mathbb{C})$

In the case of cluster manifolds associated to $PGL_n(\mathbb{C})$, the cluster seeds and tori can be represented by Thurston diagrams on a strip by superimposing two wiring diagrams, one corresponding to positive simple roots, and the other corresponding to the negative ones. The Thurston diagram description has the advantage that both the evaluation map and the the Poisson structure are easily readable from it.

Figure 1.4 and Figure 1.5 show Thurston diagrams associated to generators of the braid semigroup. The diagram corresponding to a word whose length is longer than one is obtained by gluing the diagrams associated to the generators.

It is easy to verify that the seeds obtained from a Thurston diagram corresponding to a braid semigroup generator coincide with the ones defined in subsection 1.3.1 and that gluing Thurston diagrams corresponds to the amalgamation of the corresponding

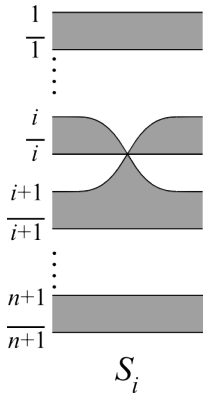

Figure 1.4: Thurston diagram corresponding to the generator s_i

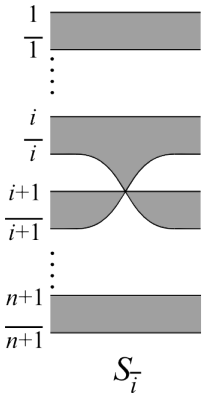

Figure 1.5: Thurston diagram corresponding to the generator $s_{\overline{i}}$

seeds. As mentioned above, the evaluation map is easily computable from a Thurston diagram corresponding to a braid semigroup element. See the following example.

Example Let us consider the word $s_1 s_{\overline{1}} s_{\overline{2}}$ in the braid semigroup of A_3. The associated Thurston diagram is depicted in Figure 1.6.

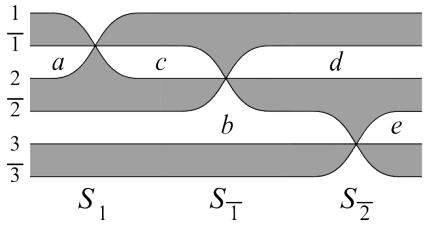

Figure 1.6: Thurston diagram associated to the word $s_1 s_{\overline{1}} s_{\overline{2}}$ in the braid semigroup of A_3.

The cluster variables are denoted by a, b, c and d. The evaluation map gives

$$H_1(a)H_2(b)E_1H_1(c)F_1F_2H_1(d)H_2(e)$$

1.5 $\widehat{A}_n$ Cluster $\mathcal{X}$-manifolds

The majority of the last section extends to the case of affine Dynkin diagrams. We present here the particular case of the $\hat{A}$ type following [FM14].

1.5.1 The coextended affine Weyl group

Let W be the type A_n Weyl group. The Weyl group W admits a central coextension $W^{\#} = W \rtimes \mathbb{Z}/N\mathbb{Z}$ generated by the simple roots $\{s_i | i \in \mathbb{Z}/N\mathbb{Z}\}$, and the additional

generator l with relations

$$\begin{aligned} s_i s_{i+1} s_i &= s_{i+1} s_i s_{i+1} && \text{for } i = 1, ..., n \\ l s_i &= s_{i+1} l && \text{for } i = 1, ..., n \\ s_i s_j &= s_j s_i && \text{for distant } i, j = 1, ..., n \\ s_i^2 &= 1 && \text{for } i = 1, ..., n \\ l^N &= 1 \end{aligned}$$

By analogy with the finite dimensional case, we introduce the braid semigroup related to $W^{\#}$. It is the semigroup freely generated by the simple roots of $W^{\#}$ and their opposites.

1.5.2 The Laurent realisation of the group $\widehat{PGL}_n^{\#}(\mathbb{C})$

In the Laurent realization, the group $\widehat{PGL}_n^{\#}(\mathbb{C})$ can be identified with the group of expressions of the form $M(\lambda)T_x$ where $M(\lambda)$ is a Laurent polynomial valued n by n matrix and T_x is the operator acting by multiplicative shift by x that is

$$T_{x_1}.M(\lambda)T_{x_2} = M(x_1\lambda)T_{x_1x_2}$$

The loop group $\widehat{PGL}_n^{\#}(\mathbb{C})$ has one more triple of generators in addition to those of PGL_n which we denote $E_0, E_{\overline{0}}$ and $H_0(x)$. In loop representation the matrices E_i for $i \neq 0, \overline{0}$ coincide with the corresponding matrices for finite-dimensional group PGL_n and the matrices $H_i(x)$ get multiplied by T_x, i.e

$$H_i(x) = \begin{pmatrix} x & 0 & & \cdots & & 0 \\ 0 & \ddots & & & & \\ & & x & & & \vdots \\ \vdots & & & 1 & & \\ & & & & \ddots & 0 \\ 0 & & \cdots & & 0 & 1 \end{pmatrix} T_x, \quad E_i = F_i^T = \begin{pmatrix} 1 & 0 & & \cdots & & 0 \\ 0 & \ddots & & & & \\ & & 1 & 1 & & \vdots \\ \vdots & & & 1 & & \\ & & & & \ddots & 0 \\ 0 & & \cdots & & 0 & 1 \end{pmatrix}$$

for $i > 0$. For $i = 0$, we additionally have $H_0(x) = T_x$ and

$$E_0 = \begin{pmatrix} 1 & 0 & \cdots & 0 \\ \vdots & \ddots & & \vdots \\ 0 & & \ddots & 0 \\ \lambda & \cdots & 0 & 1 \end{pmatrix} \qquad F_0 = \begin{pmatrix} 1 & 0 & \cdots & \lambda^{-1} \\ \vdots & \ddots & & \vdots \\ 0 & & \ddots & 0 \\ 0 & \cdots & 0 & 1 \end{pmatrix}$$

It is also useful to introduce the element $\Lambda \in \widehat{PGL}_n$ having in the loop representation the form

$$\Lambda = \begin{pmatrix} 0 & 1 & \cdots & 0 \\ \vdots & \ddots & \ddots & \vdots \\ 0 & \cdots & 0 & 1 \\ \lambda & \cdots & 0 & 0 \end{pmatrix}$$

This matrix has the property

$$E_i\Lambda = \Lambda E_{i+1}, \quad F_i\Lambda = \Lambda F_{i+1}, \quad H_i(x)\Lambda = \Lambda H_{i+1}(x), \quad i \in \mathbb{Z}/N\mathbb{Z}$$

i.e operator Λ acts as unit shift along the Dynkin diagram of $\widehat{PGL}_n$.

1.5.3 The Thurston diagram description

As in the A_n case, words in the braid semigroup of $\hat{A}$ can be represented by Thurston diagrams but, in that case, drawn on a cylinder instead of a strip. For $i \neq 0$ the Thurston diagrams are the same as in the non affine case, but viewed on a cylinder. These diagrams are shown in Figure 1.7 and Figure 1.8.

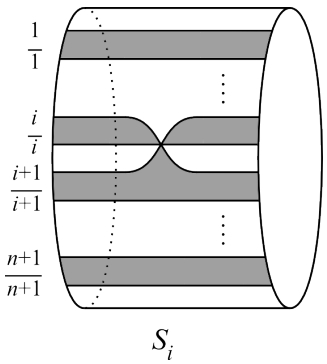

Figure 1.7: Thurston diagram corresponding to the generator s_i

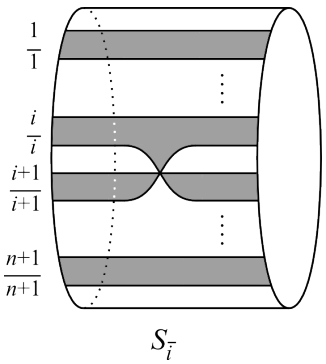

Figure 1.8: Thurston diagram corresponding to the generator $s_{\bar{i}}$

Thurston diagrams for the affine generators s_0 and $s_{\bar{0}}$ involve curves that are going "behind" the cylinder and are shown in Figure 1.9 and Figure 1.10. The Thurston diagram associated to the coextension generator l is depicted in the Figure 1.11

The seeds associated to a word in the semigroup $\widehat{\mathfrak{W}}_n$ freely generated by the s_i, $s_{\bar{i}}$ for $i \in \mathbb{Z}/n\mathbb{Z}$ and l can be determined by gluing the corresponding elementary Thurston diagrams and using the rule of the subsection 1.2.1.

Remark – The coextension generator l has no incidence on the cluster structure.

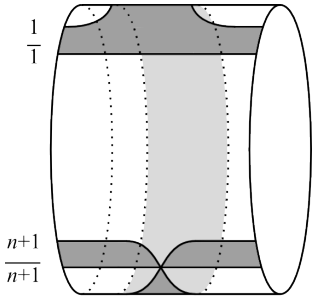

S_0

Figure 1.9: Thurston diagram corresponding to the generator s_0

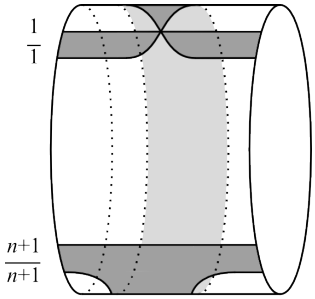

$S_{\overline{0}}$

Figure 1.10: Thurston diagram corresponding to the generator $s_{\overline{0}}$

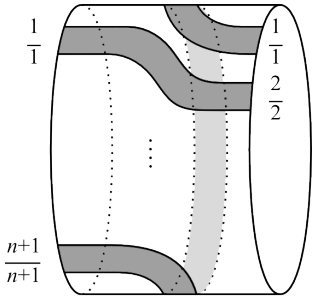

l

Figure 1.11: Thurston diagram corresponding to the coextension generator l

1.5.4 The evaluation map

The definition of the evaluation map of subsection 1.3.3 does not apply directly in the coextended affine case because of the coextension generator l. As the generator l has no incidence on the cluster seed associated to a word, one way to circumvent the novelty is to use the relation

$$ls_i = s_{i+1}l \quad \text{for } i \in \mathbb{Z}/n\mathbb{Z}$$

to move all the occurrences of l to the end (or the beginning) of the word and then use the same rule as in the non affine case and finally multiply by the group element Λ to the correct power.

Chapter 2

Links and braids

2.1 Links

We recall notions of knot theory that will be needed later. We follow the exposition of [Tur12].

A link $L \subset S^3$ is a finite set of disjoint circles embedded in S^3. These circles are called the components of L. If L is connected, it is called a knot. A link is polygonal if it is the union of a finite number of closed straight line segments. A link is tame if it is ambiently isotopic to a polygonal link. We only consider tame links. A link $L \subset \mathbb{R}^3 \subset S^3$ is usually specified by a regular projection to a plane in $\mathbb{R}^3$. We fix an orientation of S^3. A link in S^3 is ordered if its components are numbered. Let $L = L_1 \cup ... \cup L_l \subset S^3$ be an ordered link. Let $U = \coprod_{i=1}^{l} U_i$ be a regular neighborhood of L and let $E = S^3 \backslash \text{Int}(U)$ be the link exterior. Since E is a deformation retract of $S^3 \backslash L$, the group $H_1(E) = H_1(S^3 \backslash L)$ does not depend on the choice of U. We claim that this group is canonically isomorphic to a free abelian group on l generators. Indeed, the exact homology sequence of the pair (S^3, E) shows that

$$H_1(E) = H_2(S^3, E) = \bigoplus_{i=1}^{l} H_2(U_i, \partial U_i).$$

The regular neighborhood U_i of L_i can be identified with a solid torus $S^1 \times D^2$ where D^2 is a closed 2-disc. Under the identification $U_i = S^1 \times D^2$ the knot $L_i \subset U_i$ corresponds to the core $S^1 \backslash \{pt\}$ of $S^1 \times D^2$ where $pt \in \text{Int} D^2$. For any $x \in S^1$, the 2-disc $x \times D^2 \subset U_i$ meets L_i transversally in one point. We orient D^2 so that the sign of this intersection is $+$. The disc $x \times D^2$ with this orientation is called a meridional disc in U_i. The oriented loop $x \times \partial D^2 \subset \partial U_i$ is called a meridian of L_i. It is easy to see that the isotopy class of the meridian on ∂U_i neither depends on the choice of $x \in S^1$ nor on the choice of identification $U_i = S^1 \times D^2$.

The exact homology sequence of the pair $(U_i, \partial U_i)$ shows that $H_2(U_i, \partial U_i) = \mathbb{Z}$ with generator represented by a meridional disc of L_i. Therefore $H_1(E) = \mathbb{Z}t_1 \oplus ... \oplus \mathbb{Z}t_l$ where $t_i \in H_1(E)$ is the homology class of a meridian of L_i. The group ring $\mathbb{Z}[H_1(E)] =$

$\mathbb{Z}[t_1^{\pm 1}, ..., t_l^{\pm 1}]$ is the ring of Laurent polynomials in $t_1, ..., t_l$.

The group $\pi_1(E) = \pi_1(S^3 \backslash L)$ is called the group of L.

In this text we will only consider link diagrams that are connected, that is, we impose that the underlying four-valent graph is connected. Every link diagram can be transformed into a connected one with the help of the second Reidemeister move.

2.2 Milnor Torsion of link exteriors

In this section we recall the definition of the Milnor torsion of link exteriors and methods of computation of this latter. We follow the exposition of [Tur12].

2.2.1 Torsion of chain complexes

Let C be a finite acyclic based chain complex of finite dimensional vector spaces over a field $\mathbb{F}$.

$$C = (0 \to C_m \xrightarrow{\partial_{m-1}} C_{m-1} \to ... \xrightarrow{\partial_1} C_1 \xrightarrow{\partial_0} C_0 \to 0)$$

Based means that, for each C_i, we have a distinguished basis c_i.
Set $B_i = Im(C_{i+1} \xrightarrow{\partial_{i+1}} C_i) \subset C_i$. Since C is acyclic, we have the following short exact sequences:

$$0 \to B_i \hookrightarrow C_i \xrightarrow{\partial_{i-1}} B_{i-1} \to 0$$

We choose, for each i, a basis b_i of B_i. By the exactness of the previous sequence, we can complete the basis b_i to a basis of C_i by lifting elements of the basis b_{i-1}. We set

$$b_i b_{i-1} = (b_i^1, ..., b_i^k, \widetilde{b}_{i-1}^1, ..., \widetilde{b}_{i-1}^l)$$

where the $\widetilde{b}_{i-1}^j$ are lifts of the b_{i-1}^j to C_i and k and l are the dimension of B_i and B_{i-1} respectively. Let $P = (p_{ij})$ be the transition matrix from the basis c_i to the basis $b_i b_{i-1}$. We write

$$[b_i b_{i-1}/c_i] = det(P)$$

We are now ready to define the torsion of C.

Definition The torsion of C is

$$\tau(C) = \prod_{i=0}^{m} [b_i b_{i-1}/c_i] \in \mathbb{F}^*$$

Remark – The torsion depends on the distinguished basis c_i but not on the choice of the b_i.

Computation of the torsion with the method of matrix τ-chains

Throughout this section, we fix an acyclic based finite dimensional chain complex

$$C = (0 \to C_m \xrightarrow{\partial_{m-1}} C_{m-1} \to ... \xrightarrow{\partial_1} C_1 \xrightarrow{\partial_0} C_0 \to 0)$$

Let A_i be the matrix of the chain homomorphism $\partial_i : C_{i+1} \to C_i$

$$A_i = (a^i_{jk})_{\substack{j=1,...,\dim C_i \\ k=1,...,\dim C_{i+1}}}$$

Definition A *matrix chain* for C is a collection of sets $\alpha = (\alpha_0, \alpha_1, ..., \alpha_m)$, where $\alpha_i \subset \{1, 2, ..., \dim C_i\}$, so that $\alpha_0 = \emptyset$. We think of α_i as a set of basis vectors of C_i.

Let $S_i = S_i(\alpha)$ be the submatrix of A_i formed by the entries a^i_{jk} with $k \in \alpha_{i+1}$ and $j \notin \alpha_i$. The matrix chain α is called a *τ-chain* if $S_0, S_1, ..., S_{m-1}$ are square matrices. The τ-chain α is said to be *non-degenerate* if $\det S_i \neq 0$ for all i.

Proposition 2.1 *Let $\alpha = (\alpha_0, \alpha_1, ..., \alpha_m)$ be a non-degenerate τ-chain for C. Then*

$$\tau(C) = \pm \prod_{i=1}^{m-1} (\det S_i(\alpha))^{(-1)^{i+1}}$$

Computation of the torsion with the method of chain contractions

The chain contraction method for the computation of the torsion could be more relevant for a cluster theoretic interpretation of our construction. Indeed, in that setting, we can express the torsion as the determinant of an operator from black vertices to white vertices, or the opposite. The only step missing is an appropriate embedding of our graph in a surface so that we could express the torsion as the dimer partition function.

2.2.2 Milnor torsion of link exteriors

Let X be a finite connected CW-complex. Fix x_0 in X and let $\pi = \pi_1(X, x_0)$ and $H = H_1(X; \mathbb{Z})$ and $G = H/\text{Tors}H$. Let $p : \bar{X} \to X$ be the covering of X corresponding to the morphism $\pi \to G$ this covering is called the maximal free abelian covering of X. We endow $\bar{X}$ with the CW-structure induced from X. We orient all open cells of X and orient the cells of $\bar{X}$ in such a way that the restriction of p to each cell is orientation preserving. The action of H on $\bar{X}$ by covering transformations induces an action of G on the cellular chain groups $C_k(\bar{X})$. Extend this action linearly to an action of $\mathbb{Z}[G]$. In this way, $C_k(\bar{X})$ becomes a $\mathbb{Z}[G]$-module. Note that the boundary homomorphism $\partial : C_k(\bar{X}) \to C_{k-1}(\bar{X})$ is linear over $\mathbb{Z}[G]$ for all $k \geq 1$. Let $\{e^k_i\}$ be the set of oriented k-cells of X ordered in an arbitrary way. Choose over each e^k_i a k-cell $\bar{e}^k_i$ in $\bar{X}$. Then the set $\{\bar{e}^k_i\}$ is a basis of $C_k(\bar{X})$, i.e.,

$$C_k(\bar{X}) = \bigoplus_i \mathbb{Z}[G]\bar{e}^k_i.$$

Thus, $C(\bar{X})$ is a free and based chain complex over $\mathbb{Z}[G]$. Let $Q(G)$ be the quotient field of $\mathbb{Z}[G]$. Let us consider the following chain complex :

$$C = Q(G) \underset{\mathbb{Z}[G]}{\bigotimes} C(\bar{X})$$

Definition If $H_\star(C) = 0$ then the *Milnor torsion* of X is the torsion $\tau_\mu(X) = \tau(C) \in Q(G)/\pm G$.

Definition The fundamental groupoid of a topological space X is a category whose objects are the points of X and whose morphisms are endpoint-preserving homotopy classes of paths in X.

Definition A local coefficients system on X is a functor from the fundamental groupoid of X to the category of abelian groups.

Every morphism $\pi_1(X, x_0) \to G$ of the fundamental group of X to an abelian group gives rise to an isomorphism class of a local coefficient system whose fiber is isomorphic to $\mathbb{Z}[G]$, the group ring of G.

Definition The Milnor torsion of a link exterior is the torsion of the relative cellular chain complex of $(X, \partial X)$ in a local coefficients system induced by the abelianization morphism $\pi \to H \to Q(H)$.

2.3 Braids

2.3.1 The Artin braid groups

In this subsection we recall the different definitions of the braid groups. We mainly follow [KT08].

Algebraic definition

We give an algebraic definition of the braid group B_n for n a positive integer, formulated in terms of a group presentation by generators and relations.

Definition The Artin braid group B_n is the group generated by $n-1$ generators $\sigma_1, \sigma_2, \ldots, \sigma_{n-1}$ subject to the relations

$$\begin{aligned} \sigma_i\sigma_j &= \sigma_j\sigma_i && \text{for all } i,j \ = 1,2,\ldots,n-1 \text{ with } |i-j| \geq 2 \\ \sigma_i\sigma_{i+1}\sigma_i &= \sigma_{i+1}\sigma_i\sigma_{i+1} && \text{for all } i = 1,2,\ldots,n-2 \end{aligned}$$

Remark – This presentation can be recovered from the A_{n-1} Dynkin diagram

Let $\beta \in B_n$, let us define an *algebraic representative* of β to be an element of $\mathfrak{F}_{2(n-1)}$ the semigroup freely generated by $\sigma_1, \sigma_1^{-1}, \sigma_2, \sigma_2^{-1}, \ldots, \sigma_{n-1}, \sigma_{n-1}^{-1}$

Geometric braids

We give the geometric definition of the braid groups. By a *topological interval* we mean a topological space homeomorphic to the closed interval $[0,1]$. We denote by $\mathbb{D}^2$ the open unit disc in $\mathbb{R}^2$.

Definition A geometric braid on n strings is a subset β of $[0,1]\times\mathbb{R}^2$ formed by n disjoint topological intervals called the strings of β such that the projection $[0,1]\times\mathbb{R}^2 \to [0,1]$ maps each string homeomorphically onto $[0,1]$ and

$$\beta \cap (\{0\}\times\mathbb{R}^2) = \{(0,0,1),(0,0,2),\ldots,(0,0,n)\}$$
$$\beta \cap (\{1\}\times\mathbb{R}^2) = \{(1,0,1),(1,0,2),\ldots,(1,0,n)\}$$

A *braid on n strings* is an isotopy class of geometric braids.

Given two geometric braids on n strings $\beta_1,\beta_2 \subset [0,1]\times\mathbb{D}^2$, we define their product $\beta_1\beta_2$ to be the set of points $(t,x,y) \in [0,1]\times\mathbb{R}^2$ such that $(2t,x,y) \in \beta_1$ if $0 \leq t \leq 1/2$ and $(2t-1,x,y) \in \beta_2$ if $1/2 \leq t \leq 1$. The formula $(\beta_1,\beta_2) \mapsto \beta_1\beta_2$ defines a multiplication on the set of braids on n strings.

Braid diagrams

We will give a definition of braid diagram slightly stronger than usual in order to have a bijective correspondence between braid diagrams on n strands and algebraic representatives of elements of the braid group B_n.

A *braid diagram* on n strands is a set $\mathcal{D} \subset [0,1]\times\mathbb{R}$ split as a union of n topological intervals called the *strands* of $\mathcal{D}$ such that the following conditions are met:

1. The projection $[0,1]\times\mathbb{R} \to [0,1]$ maps each strand homeomorphically onto $[0,1]$
2. Every point of $\{0,1\}\times\{1,2,\ldots,n\}$ is the endpoint of a unique strand.
3. Every point of $[0,1]\times\mathbb{R}$ belongs to two strands at most . At each intersection point of two strands, these strands meet transversally and one of them is distinguished and said to be *undergoing*, the other strand being *overgoing*.
4. The projection $[0,1]\times\mathbb{R} \to [0,1]$ maps each intersection points to a different point of $[0,1]$.

Remark – The usual definition of a braid diagram is a set $\mathcal{D}$ as above satisfying only the first three conditions.

We can consider braid diagrams as a special case of graphs with additional structure describing the nature of the crossings. We call *half-arc* of a braid diagram an edge of the underlying graph. There are two types of half arcs. *Terminal half arcs* corresponding to an edge of the underlying graph having a univalent vertex and *inner half arcs* whose underlying edge connects two four-valent vertices.

2.3.2 Colored oriented braids groupoid

A *colored oriented braid on n strings* is a braid on n strings called the *underlying braid* with the additional data of a function which assigns an orientation and an integer for each string. Diagrammatically, a colored braid is a classical braid with a labeling of each strand with an integer and an arrow indicating the orientation. Multiplication is allowed if the labellings and orientations coincide.

Weighted braid diagrams

We will call weighted braid diagram a braid diagram in the sense of the previous definition with the assignment of a variable for each half-arc of the diagram.

2.3.3 Annular braid group

Geometric definition

Annular braids can be defined in a way similar to the classical braids. Let $\mathbf{A}$ be an annulus, $\mathbf{A} = \mathbb{S}^1 \times [-1, 1]$, a geometric annular braid on n strands is a set $\beta \subset \mathbf{A} \times I$ formed by n disjoint topological intervals called the strands of β such that each strand is mapped homeomorphically onto I by the projection $\mathbf{A} \times I \to I$ and

$$\beta \cap (\mathbf{A} \times \{0\}) = \{(e^{\frac{2ik\pi}{n}}, 0, 0) \; ; \; k = 0, 1, ..., n-1\}$$
$$\beta \cap (\mathbf{A} \times \{1\}) = \{(e^{\frac{2ik\pi}{n}}, 0, 1) \; ; \; k = 0, 1, ..., n-1\}$$

Examples of geometric annular braids are shown in Figure 2.1. An annular braid is an isotopy class of geometric annular braids. Composition of annular braids is defined by gluing the thickened cylinders, respecting the $\mathbb{S}^1$ coordinates.

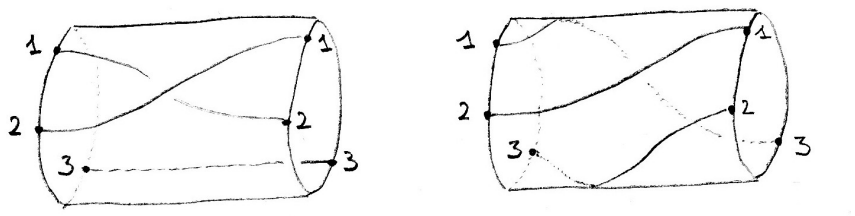

Figure 2.1: Examples of annular braids. On the left, the generator σ_1 and on the right τ^{-1}

Algebraic definition

The annular braid group is generated by

$$\sigma_1, ..., \sigma_n, \tau$$

and is ubject to the relations

$$\begin{aligned} \sigma_i\sigma_j &= \sigma_j\sigma_i && \text{for distant } i, j = 1, ..., n \\ \sigma_i\sigma_{i+1}\sigma_i &= \sigma_{i+1}\sigma_i\sigma_i && \text{for } i \in \mathbb{Z}/n\mathbb{Z} \\ \sigma_i\tau &= \tau\sigma_{i+1} && \text{for } i \in \mathbb{Z}/n\mathbb{Z} \end{aligned}$$

This presentation coincides with the presentation of the coextended affine type A braid group obtained from the type $\widehat{A}$ Dynkin diagram. The latter is a necklace with n nodes and the coextension generator ρ is the automorphism of diagram which rotates it by an angle of $\frac{2\pi}{n}$. From now on we will denote by $B^{\#}_{\widehat{A}_{n-1}}$ the annular braid group.

This group injects into the braid group on $n+1$ strands. Indeed, the annular braid group on n strands $B^{\#}_{\widehat{A}_{n-1}}$ is isomorphic to D_{n+1} which is the subgroup of the classical braid group on $n+1$ strands for which the strand beginning in position one also ends in position one. The first strand in the D_{n+1} picture corresponds to the core of the cylinder in the annular picture. For the demonstration that these group coincide (and coincide with the braid group of type B_n) we refer to the paper of Kent and Peifer [KIP02]. The D_{n+1} point of view is convenient to define the Burau representation of annular braids.

2.3.4 Colored oriented annular braids groupoid

A colored oriented annular braid on n strands is an annular braid with the additional choice for each strand of a color, that is an integer between 1 and n, and an orientation, or equivalently a sign. Composition of colored oriented annular braids is allowed if the colors and orientation coincide. The inverse of a colored oriented annular braid is given by the inverse of the underlying annular braid with the same coloring and orientations. This endows the colored oriented braids on n strands with the structure of a groupoid.

2.4 Burau representations

2.4.1 The Burau representations of colored oriented Artin braids

The reduced Burau representation

Let T be a colored oriented braid on n strands and $N(T)$ an open tubular neighborhood of T in the cylinder $D^2 \times [0,1]$, we denote by X the exterior of T.

$$X := (D^2 \times [0,1]) - N(T)$$

Let $lk(c, c')$ be the linking number of the curves c and c'. We denote by $cl(s)$ the closure of the strand s and by S_i the set of the strands of T colored with i

$$S_i := \{\text{strands of } T \text{ colored with } i\}$$

Let $\pi_1(X)$ be the fundamental group of X and ϕ the morphism from $\pi_1(X)$ which counts the total linking number of a closed curve around (the closure of) the strands marked with the same color.

$$\phi : \pi_1(X) \to \mathbb{Q}(t_1, u_1, ..., t_n, u_n)$$
$$[\gamma] \mapsto \prod_{i=1}^{n} (t_i u_i)^{k_i}$$

where $k_i := \sum_{s \in S_i} lk(\gamma, cl(s))$. The application ϕ induces an isomorphism class $\mathcal{L}$ of local coefficients system on X.

Let $D_0 := X \cap (D^2 \times \{0\})$ and $D_1 := X \cap (D^2 \times \{1\})$. We denote by $\mathcal{L}_0$ and $\mathcal{L}_1$ the induced local coefficients systems on D_0 and D_1 respectively. We define $X_{01} := (\partial D^2 \times [0,1] \cup \overline{N(T)})$. The inclusions $i_0 : (D_0, \partial D_0) \to (X, X_{01})$ and $i_1 : (D_1, \partial D_1) \to (X, X_{01})$ are homotopy equivalences and thus induce isomorphisms in homology.

$$H_1(D_0, \partial D_0; \mathcal{L}_0) \xrightarrow{(i_o)_*} H_1(X, X_{01}; \mathcal{L}) \xleftarrow{(i_1)_*} H_1(D_1, \partial D_1; \mathcal{L}_1)$$

Definition We define the reduced Burau representation of colored oriented braids as $T \mapsto (i_0)_*^{-1} \circ (i_1)_*$

Chapter 3

Cluster manifolds associated to links, braids and their invariants

3.1 Dimer model for the torsion of link exteriors

3.1.1 Introduction

We reinterpret and extend the dimer model for the Alexander polynomial of knots of Cohen, Dasbach and Russel [CDR14] to the Milnor torsion of link exteriors.

Let $L = \bigcup_{i=1}^{n} K_i$ be a colored oriented link in $\mathbb{S}^3$ and $X := \mathbb{S}^3 - N(L)$ its exterior. We denote by D_L an arbitrary connected diagram of L, that is a regular projection of L on $\mathbb{S}^2$ such that the underlying quadrivalent graph is connected. We construct an application

$$D_L \mapsto (\Gamma \xrightarrow{i} X)$$

which assigns to D_L a bipartite graph Γ embedded in X. The graph Γ can be viewed as a subgraph of the 1-skeleton of the first barycentric subdivision $S\mathcal{C}$ of a cellular decomposition $\mathcal{C}$ of $(X, \partial X)$ naturally constructed from the diagram D_L. The vertices of Γ are the barycenters of the cells of $\mathcal{C}$. The edges of Γ are the 1-cells of $S\mathcal{C}$ which connect the barycenters of the cells of $\mathcal{C}$. The bipartition of the set of vertices of Γ comes from the parity of the dimension of the cells of $\mathcal{C}$.

The bipartite graph constructed by Cohen, Dasbach and Russel is the subgraph of Γ corresponding to the 2-skeleton of the cellular decomposition.

Let ϕ be the abelianization morphism of the fundamental group of X

$$\begin{aligned} \pi_1(X) &\xrightarrow{\phi} \mathbb{Z}^n \\ \gamma &\mapsto \prod_{i=1}^{n} t_i^{k_i} \end{aligned}$$

where k_i denotes the linking number of the loop γ with the component K_i of L. The image of ϕ by the morphism induced in cohomology by the graph embedding i gives an element

$$i^*(\phi) \in H^1(\Gamma; \mathbb{Q}(t_1, \ldots, t_n))$$

We compute the Milnor torsion of X from Γ and $i^*(\phi)$. Let $\mathcal{L}$ be a local coefficients system on X induced by ϕ. The Milnor torsion of X is the torsion of the acyclic chain complex $(C_*(\mathcal{C}; \mathcal{L}), \partial_*)$. We have

$$C_*(\mathcal{C}; \mathcal{L}) \simeq C^0(\Gamma; \mathbb{Q}(t_1, \ldots, t_n))$$

and the differential ∂_* is determined by a lift of $i^*(\phi)$ to $C^1(\Gamma; \mathbb{Q}(t_1, \ldots, t_n))$.

The computation of the torsion from this data by the method of τ-chains [Tur86] extends the dimer model for the Alexander polynomial of [CDR14] in the following sense : the algorithm of Cohen, Dasbach and Russel consists, from our point of view, in a particular choice of lift of $i^*(\phi)$ and a particular choice of τ-chain.

The computation by the method of chain contractions [Coh73] enables to express the torsion of X as a dimer partition function.

3.1.2 A CW-complex structure on a link complement

Starting from a regular projection of a link, we endow the link exterior with the strucure of a CW-complex. We will simultaneously construct the CW-complex structure on the interior and the boundary of X, however the cell structure on the latter is not important since we will mod the boundary out in our computations. The 1-skeleton of the CW-complex structure on the link exterior and part of the image of the attaching map of a 2-cell corresponding to a region of the diagram are depicted in Figure 3.1.

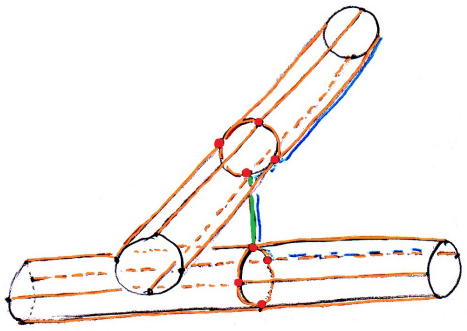

Figure 3.1: The 1-skeleton of the CW-complex structure on the link exterior and part of the image of the attaching map of a 2-cell corresponding to a region of the diagram

0-cells

We consider eight 0-cells for each crossing of the diagram as can be seen in the Figure 3.1. All of the 0-cells are on the boundary of X. The 0-cells are depicted in red in figure 3.1.

1-cells

Each crossing gives eight 1-cells on ∂X. We add $4n$ 1-cells on ∂X, where n stands for the half arcs of the link diagram, that is, the number of edges of the underlying four-valent graph. In the interior of X, for each crossing of the link diagram we add a vertical 1-cell joining the torus under the projection plane and the torus above it and we orient them upwards. The 1-cells of our decomposition of ∂X are depicted in orange, and the 1-cells which belong to the interior are depicted in green in Figure 3.1.

2-cells

We complete the cellular decomposition of ∂X, which is a union of tori, for that we need four 2-cells per half-arc of the link diagram. In the interior of X we glue a 2-cell for each region of the link diagram (that is each complementary region in the plane of the quadrivalent graph corresponding to the link projection). We glue them in each region following the boundary of the link exterior and following our previously added 1-cells at the crossings. In Figure 3.1 a part of the image of the attaching map of a 2-cell corresponding to a region of the diagram is depicted in blue.

3-cells

We eventually need to glue two 3-cells, one under the projection plane and one over. Attaching maps of the 3-cells near a crossing are described in the Figure 3.2.

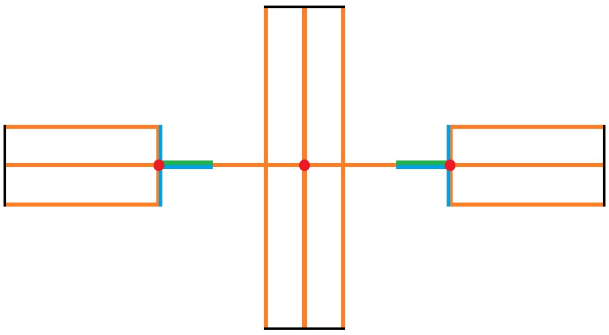

Figure 3.2: Attaching maps of the 3-cells near a crossing

3.1.3 Graph encoding the cellular structure

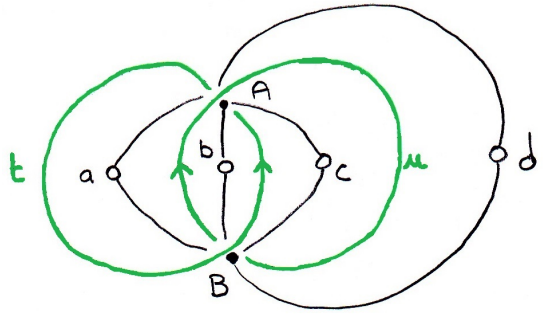

Figure 3.3: Link diagram and associated bipartite graph encoding the 2-skeleton of the relative cellular structure.

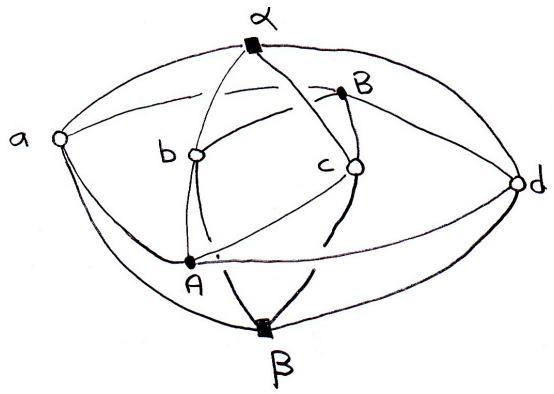

Figure 3.4: Bipartite graph associated to a link diagram.

In this subsection we will construct a bipartite graph encoding the CW-complex structure on the link exterior modulo its boundary $(X, \partial X)$ described above. The Hopf Link will serve as an example. We start with an oriented and ordered link diagram. Recall that we impose that the diagram is connected.

Black vertices

We put a (round) black vertex for each 1-cell of our cellular decomposition, that is at crossings of the link diagram. And (square) black vertices for the 3-cells.

White vertices

We put a white vertex for each region of the diagram, that is, for each connected component of the complementary in the plan of projection of the underlying four-valent graph.

Edges

We put an edge between a white vertex and a black vertex if the corresponding crossing and region are adjacent. Edges are oriented from white to black vertices.

From this point of view. The bipartite graph constructed by Cohen, Dasbach and Russel is the subgraph corresponding to the 2-skeleton of the cellular decomposition of the link exterior relative to its boundary. See Figure 3.3 for the subgraph and Figure 3.4 for the complete graph, both in the case of the usual Hopf link diagram.

3.1.4 Weighting on the graph

We will assign weights to edges of our graph Γ with values in the free abelian group generated by $t_1, ..., t_l$, that is the weighting may be viewed as an element of $C_1(\Gamma, \mathbb{Z}^l)$. The weighting on Γ is induced by the embedding $\Gamma \subset E$. Consider the cellular cochain complex of Γ with coefficients in $\mathbb{Z}^l$.

$$0 \to C^0(\Gamma, \mathbb{Z}^l) \xrightarrow{\delta} C^1(\Gamma, \mathbb{Z}^l) \to 0$$

We have $H^1(\Gamma, \mathbb{Z}^l) = C^1(\Gamma, \mathbb{Z}^l)/\delta C^0(\Gamma, \mathbb{Z}^l)$ and by the universal coefficient theorem $H^1(\Gamma, \mathbb{Z}^l) = \text{Hom}(H_1(\Gamma, \mathbb{Z}^l))$. The weighting we are interested in is a lift to $C^1(\Gamma, \mathbb{Z}^l)$ of the cocycle of $H^1(\Gamma, \mathbb{Z}^l)$ iduced by the inclusion $\Gamma \xrightarrow{i} E$.

$$\begin{aligned} H_1(\Gamma) &\xrightarrow{i_*} H_1(E) \simeq \mathbb{Z}^l \\ c &\mapsto t_1^{\text{lk}(c,L_1)} ... t_l^{\text{lk}(c,L_l)} \end{aligned}$$

Suppose our link has n components, we assign a variable $t_1, t_2, ..., t_n$ to each component. In our example, in Figure 3.3, these variables are t and u. Now we will put weights on our graph. These weights will encode a local coefficients system induced by the abelianization morphism from the fundamental group of the link to the free abelian group on n generators :

$$\begin{aligned} \rho : \pi_1(X) &\to \langle t_1, t_2, ..., t_n \rangle \\ \gamma &\mapsto \text{lk}(L, \gamma) \end{aligned}$$

It can also be interpreted as a choice of a lift of each cell of our cellular decomposition of the link exterior in the maximal abelian cover of this latter. We orient our graph from white vertices to black vertices. We want to weight the graph so that the product of the weights along an oriented cycle c, where we take the inverse of the edge variable if we travel along the edge against its orientation, to be equal to its homology class, $\text{lk}(c, K)$. To do so, we can choose a maximal tree in our graph, as in Figure 3.5 where the maximal tree is depicted in orange, we assign the weight 1 to all the edges of the

maximal tree and label the remaining edges with the weight satisfying the preceding rule. We illustrate this in the example in Figure 3.6 and Figure Figure 3.7.

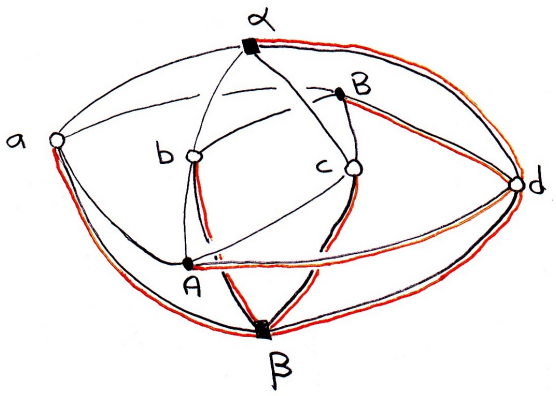

Figure 3.5: A maximal tree in the bipartite graph.

We have splitted the graph in two as it turns out that they will correspond respectively to ∂_1 and ∂_2 in the cellular chain complex $C_*(X, \partial X; E)$ of the link exterior modulo its boundary in a local coefficients system E determined by ρ. In these figures, orange edges correspond to the maximal tree, green variables correspond to the homology class of the cycles corresponding to the faces in which they are and blue variables are the weights assigned to the edges so that our rule is followed.

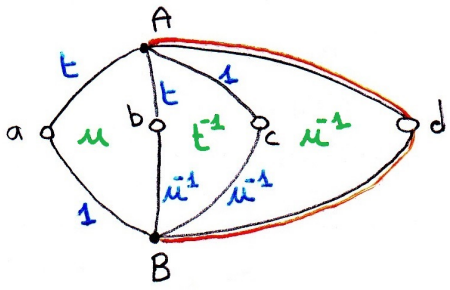

Figure 3.6: Weights corresponding to ∂_1

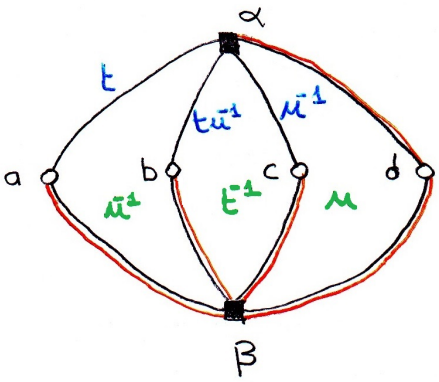

Figure 3.7: Weights corresponding to ∂_2

3.1.5 Computation of the torsion of the link exterior

We present here two methods of computation of the torsion of a link exterior from the weighted bipartite graph previously constructed. The first one is the method of τ-chains and the second one, the method of chains contractions. The τ-chain point of view is useful to understand of the transition from links to braids, whereas the chain contraction point of view is best suited for a cluster theoretic of the torsion of link

exteriors as this latter can be expressed as a dimer partition function.

τ-chains

We have the following cellular chain complex $C = C_*(X, \partial X; E)$ of the link exterior modulo its boundary with a local coefficients system determined by the abelianization morphism.

$$C = (0 \to C_3 \xrightarrow{\partial_2} C_2 \xrightarrow{\partial_1} C_1 \to 0)$$

We can determine the matrices A_i of the ∂_i from the bipartite graph. In our example, in the basis $\{\alpha, \beta\}$ of C_3, $\{a, b, c, d\}$ of C_2 and $\{A, B\}$ of C_1, the matrices are given by :

$$A_2 = \begin{pmatrix} t^{-1} & 1 \\ t^{-1}u & 1 \\ u & 1 \\ 1 & 1 \end{pmatrix} \qquad A_1 = \begin{pmatrix} -t & t & -1 & 1 \\ -1 & u^{-1} & -u^{-1} & 1 \end{pmatrix}$$

Now let us consider the τ-chain $\alpha = (\alpha_3, \alpha_2, \alpha_1)$ where $\alpha_3 = \{\alpha, \beta\}$ $\alpha_2 = \{b, d\}$ and $\alpha_1 = \{\emptyset\}$. With this τ-chain we have :

$$S_2(\alpha) = \begin{pmatrix} t^{-1} & 1 \\ u & 1 \end{pmatrix} \qquad S_1(\alpha) = \begin{pmatrix} t & 1 \\ u^{-1} & 1 \end{pmatrix}$$

3.2 Burau cluster submanifolds associated to braids

In this section, we associate to colored oriented braid representatives, pairs consisting of a cluster $\mathcal{X}$-manifold related to the type A_n braid semigroup and a submanifold of the latter.

More precisely, we construct two maps ψ^r and ψ^u, the first one from the set of representatives of colored oriented braids on n strands, Br_n^c, to the set of pairs $\{(M_{A_n}, S)\}$ consisting of an A_n type cluster $\mathcal{X}$-manifold and a submanifold of it. And the second one from Br_n^c to the set of pairs $\{(M_{A_{n-1}}, S)\}$ consisting of an A_{n-1} type cluster $\mathcal{X}$-manifold and a submanifold of it.

$$Br_n^c \xrightarrow{\psi^r} \{(\mathcal{X}_{A_n} - \text{manifold},\ \text{submanifold})\} \tag{3.1}$$

$$Br_n^c \xrightarrow{\psi^u} \{(\mathcal{X}_{A_{n-1}} - \text{manifold},\ \text{submanifold})\} \tag{3.2}$$

The map ψ^r can be viewed as a translation in the context of braids of the construction in section 3.1.

By construction, these maps respect the multiplications in the sense that, to a product of colored braid representatives corresponds the multiplication of the associated cluster manifolds and its restriction to the submanifolds.

The composition of these maps with the evaluation map restricted to the submanifolds is independent of the chosen representatives and gives projective versions of the generalized reduced and unreduced Burau representations respectively.

In subsection 3.2.1 we construct the map ψ^r and prove the following theorem.

Theorem 3.1 *For $n \geq 3$, let $\rho : B_n^c \to GL_{n+1}(\mathbb{Q}(t_1, u_1, \ldots, t_n, u_n))$ be the composition of the map r, which assigns an arbitrary representative to colored oriented braid, with ψ^r and the evaluation map restricted to the second factor :*

$$\rho : B_n^c \xrightarrow{r} Br_n^c \xrightarrow{\psi^r} \{(M_{A_n}, S)\} \xrightarrow{ev_{|S}} GL_{n+1}(\mathbb{Q}(t_1, u_1, \ldots, t_n, u_n))$$

The map ρ is a representation of the colored oriented braid groupoid on n strands, which coincides with the generalized reduced Burau representation.

In subsection 3.2.3 we construct the map ψ^u and prove the corresponding theorem.

Theorem 3.2 *For $n \geq 3$, let $\rho_u : B_n^c \to PGL_n(\mathbb{Q}(t_1, \ldots, t_n))$ be the composition of the map r, which assigns an arbitrary representative to colored oriented braid, with ψ^u and the evaluation map restricted to the second factor :*

$$\rho_u : B_n^c \xrightarrow{r} Br_n^c \xrightarrow{\psi^u} \{(M_{A_{n-1}}, S)\} \xrightarrow{ev_{|S}} PGL_n(\mathbb{Q}(t_1, \ldots, t_n))$$

The map ρ_u is a projective representation of the colored oriented braid groupoid on n strands, which coincides with the projectivization of the generalized unreduced Burau representation.

3.2.1 Burau cluster submanifolds associated to oriented colored braids, the reduced case

We construct the map ψ^r from the set of representatives of colored oriented braids on n strands to the set of pairs consisting of an A_n type cluster $\mathcal{X}$-manifold and a submanifold of it.

$$Br_n^c \xrightarrow{\psi^r} \{(\mathcal{X}_{A_n} - \text{manifold}, \text{ submanifold})\}$$

First, we define the ambient cluster $\mathcal{X}$-manifold. Algebraically by assigning to an algebraic representative of the underlying braid, an element of the braid semigroup; and diagrammatically by associating a Thurston diagram to a diagrammatic braid representative. Then we give the rule of construction of the submanifolds. In the reduced case, this rule is a translation, in the context of braids, of the construction in section 3.1.

Construction of the ambient manifold

Let β_c^r be a colored oriented braid representative on n strands and $\beta^r \in B_n$ the underlying braid representative. We associate to β^r an element of $\mathfrak{W}_n$ with the morphism of semigroups ψ defined below.

$$\begin{aligned} \psi : \mathfrak{F}_{2(n-1)} &\to \mathfrak{W}_n \\ \sigma_i &\mapsto s_{\bar{i}} s_{i+1} \\ \sigma_i^{-1} &\mapsto s_{i+1} s_{\bar{i}} \end{aligned}$$

Recall from section 1.1 that to the element $\psi(\beta^r)$ of $\mathfrak{W}_n$ corresponds a seed, $\mathcal{X}_{\mathbf{J}(\psi(\beta^r))}$, of the A_n cluster $\mathcal{X}$-manifold associated to $p(\psi(\beta^r)) \in \mathcal{B}$. Diagramatically the construction of the manifolds for the braid representatives semigoup generators translates in Figure 3.8 and Figure 3.9.

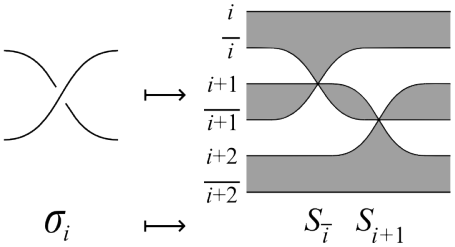

Figure 3.8: Diagrammatic rule for the construction of the ambient variety

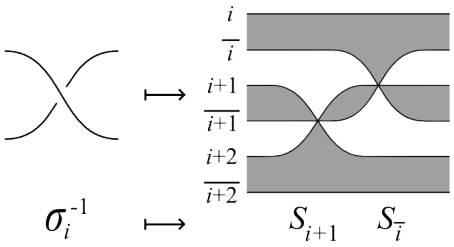

Figure 3.9: Diagrammatic rule for the construction of the ambient variety

The Thurston diagram corresponding to a braid diagram with more than one crossing is obtained by gluing the diagrams associated to the generators of B_n and their inverses.

Remark – In the particular seed tori of the cluster manifolds we have constructed the cluster variables correspond to half arcs of the underlying braid representative.

Construction of the submanifold

We construct in the particular seed associated to $\psi(\beta^r)$ a submanifold. As mentioned above, in that particular seed, the cluster variables correspond to half arcs of the braid diagram. The rule of construction of the submanifold is reminiscent of the construction of section 3.1. The parametrization for the submanifolds is described in Figure 3.10 and Figure 3.11.

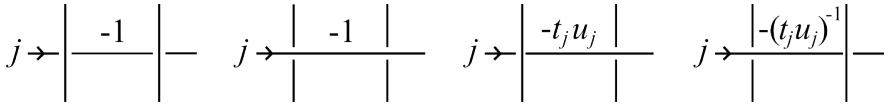

Figure 3.10: Submanifold parameters for internal half arcs.

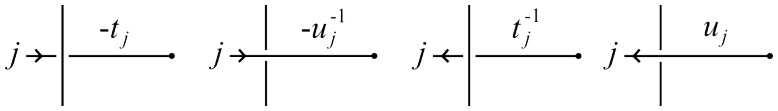

Figure 3.11: Submanifold parameters for terminal half arcs.

3.2.2 Demonstration of theorem 3.1

As the map ψ^r is compatible with the multiplications, the fact that ρ is a representation will follow from its independence of the chosen representative.

Let (β, c) be a colored oriented braid on n strands and, (β_1^r, c) and (β_2^r, c) two representatives of it. From the algebraic point of view, β_1 and β_2 are words in the alphabet $\{\sigma_1, \ldots, \sigma_{n-1}, \sigma_1^{-1}, \ldots, \sigma_{n-1}^{-1}\}$ that can be obtained from one another using the relations

$$\begin{aligned}
\sigma_i\sigma_j &= \sigma_j\sigma_i && \text{for all } i,j = 1,2,\ldots,n-1 \text{ with } |i-j| \geq 2\\
\sigma_i\sigma_{i+1}\sigma_i &= \sigma_{i+1}\sigma_i\sigma_{i+1} && \text{for all } i = 1,2,\ldots,n-2\\
\sigma_i\sigma_i^{-1} &= 1 && \text{for all } i = 1,2,\ldots,n-1\\
\sigma_i^{-1}\sigma_i &= 1 && \text{for all } i = 1,2,\ldots,n-1
\end{aligned}$$

Based on the fact that both ψ^r and the evaluation map are compatible with the multiplications, it suffices to show that

$$\begin{aligned}
ev_{|S} \circ \psi^r(\sigma_i\sigma_j, c) &= ev_{|S} \circ \psi^r(\sigma_j\sigma_i, c) && \text{for all } i,j = 1,2,\ldots,n-1 \text{ with } |i-j| \geq 2\\
ev_{|S} \circ \psi^r(\sigma_i\sigma_{i+1}\sigma_i, c) &= ev_{|S} \circ \psi^r(\sigma_{i+1}\sigma_i\sigma_{i+1}, c) && \text{for all } i = 1,2,\ldots,n-2\\
ev_{|S} \circ \psi^r(\sigma_i\sigma_i^{-1}, c) &= ev_{|S} \circ \psi^r(1, c) && \text{for all } i = 1,2,\ldots,n-1\\
ev_{|S} \circ \psi^r(\sigma_i^{-1}\sigma_i,) &= ev_{|S} \circ \psi^r(1, c) && \text{for all } i = 1,2,\ldots,n-1
\end{aligned}$$

In fact, we are going to show that

$$\begin{aligned}
\psi^r(\sigma_i\sigma_j, c) &= \psi^r(\sigma_j\sigma_i, c) && \text{for all } i,j = 1,2,\ldots,n-1 \text{ with } |i-j| \geq 2\\
\psi^r(\sigma_i\sigma_{i+1}\sigma_i, c) &= \psi^r(\sigma_{i+1}\sigma_i\sigma_{i+1}, c) && \text{for all } i = 1,2,\ldots,n-2
\end{aligned}$$

Invariance under commuting relations

Invariance under commuting relations, or diagrammatically, isotopy invariance, is a consequence of the first and second items of theorem 1.1 in subsection 1.3.4. That is the seeds we associate to braid representatives related by commuting relations are isomorphic. Let us consider i and j with $|i-j| \geq 2$. We have :

$$\psi(\sigma_i\sigma_j) = s_{\bar{i}}s_{i+1}s_{\bar{j}}s_{j+1}$$
$$\psi(\sigma_j\sigma_i) = s_{\bar{j}}s_{j+1}s_{\bar{i}}s_{i+1}$$

The corresponding words in the braid semigroup are related by the following sequence of relations which, according to theorem 1.1, induce isomorphisms of the corresponding seeds.

$$s_{\bar{i}}s_{i+1}s_{\bar{j}}s_{j+1} \to s_{\bar{i}}s_{\bar{j}}s_{i+1}s_{j+1} \to s_{\bar{i}}s_{\bar{j}}s_{j+1}s_{i+1} \to s_{\bar{j}}s_{\bar{i}}s_{j+1}s_{i+1} \to s_{\bar{j}}s_{j+1}s_{\bar{i}}s_{i+1}$$

This shows that, independently of the coloring function c, we have

$$\psi^r(\sigma_i\sigma_j, c) = \psi^r(\sigma_j\sigma_i, c) \text{ for all } i, j \ = 1, 2, \ldots, n-1 \text{ with } |i-j| \geq 2$$

and thus, invariance under commuting relations.

At the level of GL_n, invariance under isotopy is a consequence of the commuting relations of the group generators E_i, E_j, F_i and F_j where $|i-j| \geq 2$. Indeed, suppose that we have an algebraic representative of the underlying braid of a colored oriented braid of the form $\sigma_i\sigma_j$ with $|i-j| \geq 2$, then the associated element of the braid semigroup is given by

$$\psi(\sigma_i\sigma_j) = s_{\bar{i}}s_{i+1}s_{\bar{j}}s_{j+1}$$

Independently of the subvariety parameters, the evaluation map on the associated seed torus gives

$$H(a)F_iE_{i+1}F_jE_{j+1}H'(b) = H(a)F_jE_{j+1}F_iE_{i+1}H'(b)$$

where $H(a)$ and $H'(b)$ are elements of the Cartan subgroup. The right hand side of the last equality is the result of the evaluation map on the seed torus corresponding to

$$s_{\bar{j}}s_{j+1}s_{\bar{i}}s_{i+1} = \psi(\sigma_{j+1}\sigma_{i+1})$$

Invariance under the third Reidemeister move

We show that :

$$\psi^r(\sigma_i\sigma_{i+1}\sigma_i, c) = \psi^r(\sigma_{i+1}\sigma_i\sigma_{i+1}, c) \qquad \text{for all } i = 1, 2, \ldots, n-2$$

We have :

$$\psi(\sigma_i\sigma_{i+1}\sigma_i) = s_{\overline{i}}s_{i+1}s_{\overline{i+1}}s_{i+2}s_{\overline{i}}s_{i+1}$$
$$\psi(\sigma_{i+1}\sigma_i\sigma_{i+1}) = s_{\overline{i+1}}s_{i+2}s_{\overline{i}}s_{i+1}s_{\overline{i+1}}s_{i+2}$$

The words $s_{\overline{i}}s_{i+1}s_{\overline{i+1}}s_{i+2}s_{\overline{i}}s_{i+1}$ and $s_{\overline{i+1}}s_{i+2}s_{\overline{i}}s_{i+1}s_{\overline{i+1}}s_{i+2}$ are equal in the braid semigroup of A_n and thus, by Theorem 1.1, the associated seeds are related by a cluster transformation and define two parametrization domains of the same cluster manifold.

It remains to show that the submanifolds associated to $(\sigma_i\sigma_{i+1}\sigma_i, c)$ and $(\sigma_{i+1}\sigma_i\sigma_{i+1}, c)$ are the same. We deal in detail with the case where the orientations of all the braided strands are positive, and the strands $i, i+1$ and $i+2$ are colored by $1, 2$ and 3 respectively, to avoid complicated notations. The other cases are easily deduced by changes of variables. The orientations and colorings of the over strands have no influence on the result. The corresponding weighted braid diagrams are depicted in Figure 3.12 and Figure 3.13 where only the braided strands are drawn.

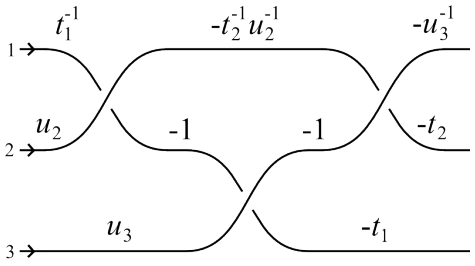

Figure 3.12: Oriented colored braid weighted diagram whose underlying algebraic braid representative is $\sigma_i\sigma_{i+1}\sigma_i$

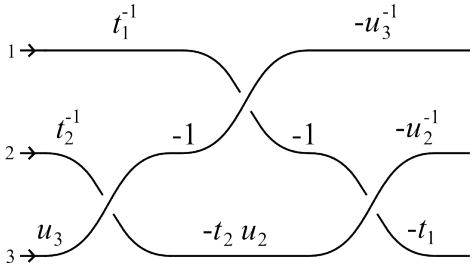

Figure 3.13: Oriented colored braid weighted diagram whose underlying algebraic braid representative is $\sigma_{i+1}\sigma_i\sigma_{i+1}$

The associated ambient cluster manifold parametrization domains are related by a cluster transformation induced by the following sequence of relations in the braid semigroup. Care must be taken with the -1 parameters as mutations in these vertices are not defined. Braces indicate where transformations occur. We indicate next to the words the nature of the transformations.

1. $\underbrace{s_{\overline{i}}s_{i+1}}\, s_{\overline{i+1}}\, \underbrace{s_{i+2}s_{\overline{i}}}\, s_{i+1}$ 2 isomorphisms
2. $s_{i+1}\, \underbrace{s_{\overline{i}}s_{\overline{i+1}}s_{\overline{i}}}\, s_{i+2}s_{i+1}$ 1 mutation
3. $\underbrace{s_{i+1}s_{\overline{i+1}}}\, s_{\overline{i}}s_{\overline{i+1}}s_{i+2}s_{i+1}$ 1 mutation
4. $s_{\overline{i+1}}s_{i+1}s_{\overline{i}}\, \underbrace{s_{\overline{i+1}}s_{i+2}}\, s_{i+1}$ 1 isomorphism

5. $s_{\overline{i+1}}s_{i+1}s_{\bar{i}}s_{i+2}\underbrace{s_{\overline{i+1}}s_{i+1}}$ 1 mutation

6. $s_{\overline{i+1}}\underbrace{s_{i+1}s_{\bar{i}}}s_{i+2}s_{i+1}s_{\overline{i+1}}$ 1 isomorphism

7. $s_{\overline{i+1}}s_{\bar{i}}\underbrace{s_{i+1}s_{i+2}s_{i+1}}s_{\overline{i+1}}$ 1 mutation

8. $s_{\overline{i+1}}\underbrace{s_{\bar{i}}s_{i+2}}s_{i+1}\underbrace{s_{i+2}s_{\overline{i+1}}}$ 2 isomorphisms

9. $s_{\overline{i+1}}s_{i+2}s_{\bar{i}}s_{i+1}s_{\overline{i+1}}s_{i+2}$

These transformations and the transformations of the submanifold parameters are represented in the following Thurston diagrams.

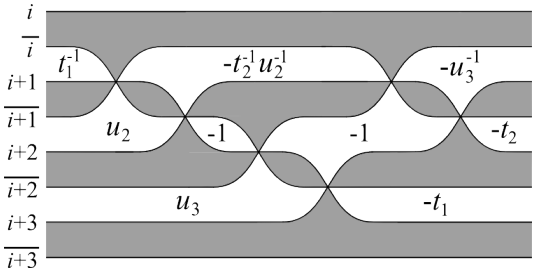

Figure 3.14: Thurston diagram description of the seed corresponding to $s_{\bar{i}}s_{i+1}s_{\overline{i+1}}s_{i+2}s_{\bar{i}}s_{i+1}$, and submanifold parameters.

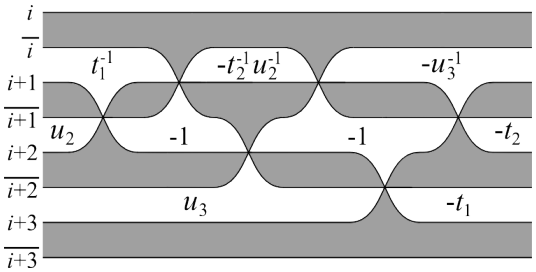

Figure 3.15: Thurston diagram description of the seed corresponding to $s_{i+1}s_{\bar{i}}s_{\overline{i+1}}s_{\bar{i}}s_{i+2}s_{i+1}$, and submanifold parameters.

This diagram is obtained from the one in Figure 3.14 by the application of two gray moves.

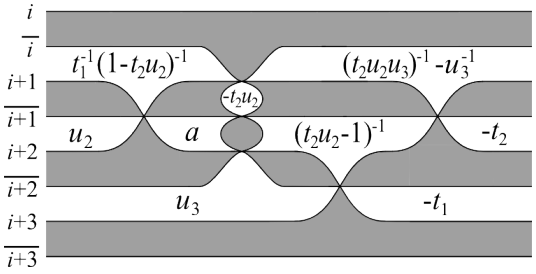

Figure 3.16: Thurston diagram obtained from the one in Figure 3.15 by a white move in the face with the variable $-t_2^{-1}u_2^{-1}$, and submanifold parameters where $a = \frac{1-t_2u_2}{t_2u_2}$.

Note that this diagram does not correspond to any word in $\mathfrak{W}$.

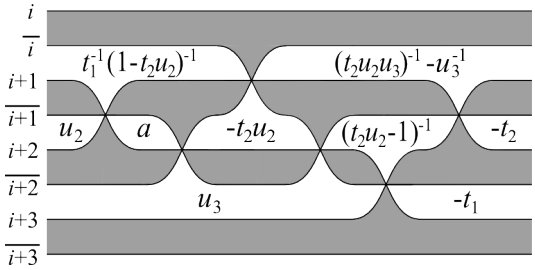

Figure 3.17: Thurston diagram description of the seed corresponding to $s_{i+1}s_{\overline{i+1}}s_{\overline{i}}s_{\overline{i+1}}s_{i+2}s_{i+1}$, and submanifold parameters where $a = \frac{1-t_2u_2}{t_2u_2}$.

This diagram is obtained from the one in Figure 3.16 by a gray move.

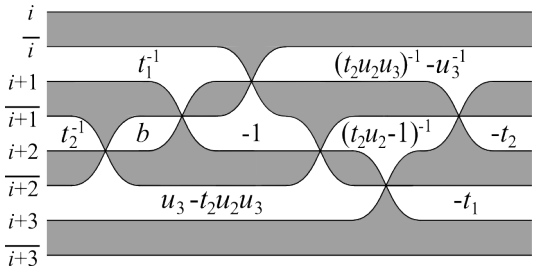

Figure 3.18: Thurston diagram description of the seed corresponding to $s_{\overline{i+1}}s_{i+1}s_{\overline{i}}s_{\overline{i+1}}s_{i+2}s_{i+1}$, and submanifold parameters where $b = \frac{t_2u_2}{1-t_2u_2}$.

This diagram is obtained from the one in Figure 3.17 by a white move in the face with the parameter a.

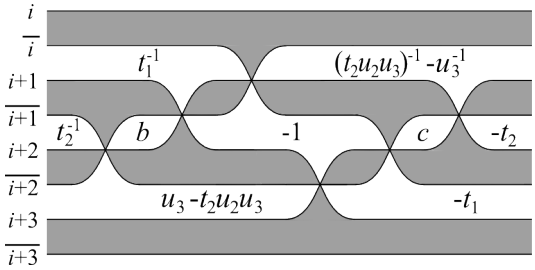

Figure 3.19: Thurston diagram description of the seed corresponding to $s_{\overline{i+1}}s_{i+1}s_{\overline{i}}s_{i+2}s_{\overline{i+1}}s_{i+1}$, and submanifold parameters where $b = \frac{t_2u_2}{1-t_2u_2}$ and $c = (t_2u_2 - 1)^{-1}$.

This diagram is obtained from the one in Figure 3.18 by a gray move.

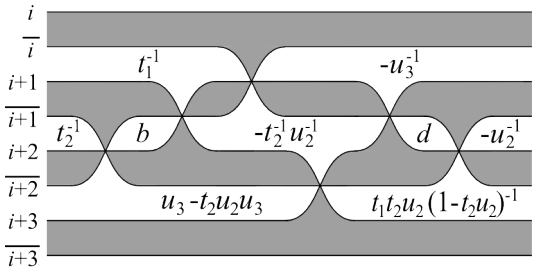

Figure 3.20: Thurston diagram description of the seed corresponding to $s_{\overline{i+1}}s_{i+1}s_{\overline{i}}s_{i+2}s_{i+1}s_{\overline{i+1}}$, and submanifold parameters where $b = \frac{t_2u_2}{1-t_2u_2}$ and $d = t_2u_2 - 1$.

This diagram is obtained from the one in Figure 3.17 by a white move in the face with the parameter c.

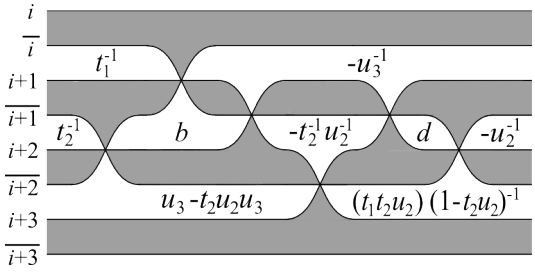

Figure 3.21: Thurston diagram description of the seed corresponding to $s_{\overline{i+1}}s_{\overline{i}}s_{i+1}s_{i+2}s_{i+1}s_{\overline{i+1}}$, and submanifold parameters where $b = \frac{t_2u_2}{1-t_2u_2}$ and $d = t_2u_2 - 1$.

This diagram is obtained from the one in Figure 3.18 by a gray move.

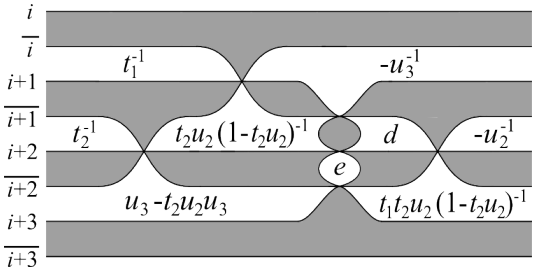

Figure 3.22: Thurston diagram obtained from the one in Figure 3.21 by a gray move, and submanifold parameters where $e = -t_2^{-1}u_2^{-1}$.

Note that this diagram does not correspond to any word in $\mathfrak{W}$.

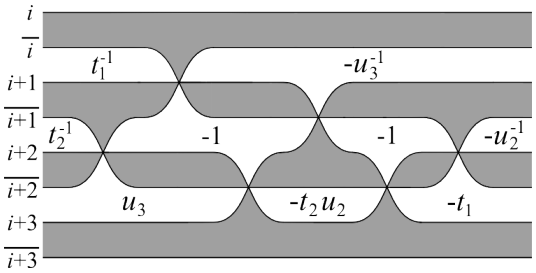

Figure 3.23: Thurston diagram description of the seed corresponding to $s_{\overline{i+1}}s_{\bar{i}}s_{i+2}s_{i+1}s_{i+2}s_{\overline{i+1}}$, and submanifold parameters.

This diagram is obtained from the one in Figure 3.22 by a white move in the face with the parameter e.

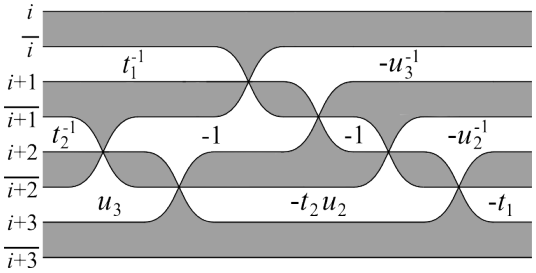

Figure 3.24: Thurston diagram description of the seed corresponding to $s_{\overline{i+1}}s_{i+2}s_{\bar{i}}s_{i+1}s_{\overline{i+1}}s_{i+2}$, and submanifold parameters.

This shows that the map ψ^r associates the same cluster manifold to braid representatives differing by a Reidemeister 3 move and the same submanifold but in a different chart.

The results of the evaluation map on the corresponding seed tori are given below, where item k is the result of the evaluation map on the submanifold associated to the colored braid representative in Figure 3.12 in the seed corresponding to the word in item k of the list beginning page 38.

1. $H_i(t_1^{-1})H_{i+1}(u_2)H_{i+2}(u_3)F_iE_{i+1}H_i(-t_2^{-1}u_2^{-1})H_{i+1}(-1)F_{i+1}E_{i+2}H_{i+1}(-1)F_i\dots$
   $\dots E_{i+1}H_i(-u_3^{-1})H_{i+1}(-t_2)H_{i+2}(-t_1)$

2. $H_i(t_1^{-1})H_{i+1}(u_2)H_{i+2}(u_3)E_{i+1}H_i\underbrace{F_iH_i(-t_2^{-1}u_2^{-1})F_{i+1}F_i}H_iE_{i+2}E_{i+1}\dots$
   $\dots H_i(-u_3^{-1})H_{i+1}(-t_2)H_{i+2}(-t_1)$

3. $H_i(\frac{t_1^{-1}}{1-t_2u_2})H_{i+1}(u_2)H_{i+2}(u_3)\underbrace{E_{i+1}H_{i+1}(\frac{1-t_2u_2}{t_2u_2})F_{i+1}}H_{i+1}(-t_2u_2)F_iF_{i+1}\dots$
   $\dots H_{i+1}(\frac{1}{t_2u_2-1})E_{i+2}E_{i+1}H_i(\frac{1-t_2u_2}{t_2u_2u_3})H_{i+1}(-t_2)H_{i+2}(-t_1)$

4. $H_i(t_1^{-1})H_{i+1}(t_2^{-1})H_{i+2}(u_3 - t_2u_2u_3)F_{i+1}H_{i+1}(\frac{t_2u_2}{1-t_2u_2})E_{i+1}H_{i+1}(-1)F_iF_{i+1}\dots$
$\dots H_{i+1}(\frac{1}{t_2u_2-1})E_{i+2}E_{i+1}H_i(\frac{1-t_2u_2}{t_2u_2u_3})H_{i+1}(-t_2)H_{i+2}(-t_1)$

5. $H_i(t_1^{-1})H_{i+1}(t_2^{-1})H_{i+2}(u_3 - t_2u_2u_3)F_{i+1}H_{i+1}(\frac{t_2u_2}{1-t_2u_2})E_{i+1}H_{i+1}(-1)F_iE_{i+2}\dots$
$\dots \underbrace{F_{i+1}H_{i+1}(\frac{1}{t_2u_2-1})E_{i+1}}\, H_i(\frac{1-t_2u_2}{t_2u_2u_3})H_{i+1}(-t_2)H_{i+2}(-t_1)$

6. $H_i(t_1^{-1})H_{i+1}(t_2^{-1})H_{i+2}(u_3 - t_2u_2u_3)F_{i+1}H_{i+1}(\frac{t_2u_2}{1-t_2u_2})E_{i+1}H_{i+1}(-t_2^{-1}u_2^{-1})F_i\dots$
$\dots E_{i+2}E_{i+1}H_{i+1}(t_2u_2-1)F_{i+1}H_i(-u_3^{-1})H_{i+1}(-u_2^{-1})H_{i+2}(\frac{t_1t_2u_2}{1-t_2u_2})$

7. $H_i(t_1^{-1})H_{i+1}(t_2^{-1})H_{i+2}(u_3 - t_2u_2u_3)F_{i+1}H_{i+1}(\frac{t_2u_2}{1-t_2u_2})F_i\dots$
$\underbrace{E_{i+1}H_{i+1}(-t_2^{-1}u_2^{-1})E_iE_{i+1}}\, H_{i+1}(t_2u_2-1)F_{i+1}H_i(-u_3^{-1})H_{i+1}(-u_2^{-1})H_{i+2}(\frac{t_1t_2u_2}{1-t_2u_2})$

8. $H_i(t_1^{-1})H_{i+1}(t_2^{-1})H_{i+2}(u_3)F_{i+1}H_{i+1}(-1)F_iE_{i+2}H_{i+2}(-t_2u_2)E_{i+1}H_{i+1}(-1)\dots$
$\dots E_{i+2}F_{i+1}H_i(-u_3^{-1})H_{i+1}(-u_2^{-1})H_{i+2}(-t_1)$

9. $H_i(t_1^{-1})H_{i+1}(t_2^{-1})H_{i+2}(u_3)F_{i+1}E_{i+2}H_{i+1}(-1)H_{i+2}(-t_2u_2)F_iE_{i+1}H_{i+1}(-1)\dots$
$\dots F_{i+1}E_{i+2}H_i(-u_3^{-1})H_{i+1}(-u_2^{-1})H_{i+2}(-t_1)$

Invariance under the second Reidemeister move

Invariance under the second Reidemeister move is a consequence of the following relations between the generators of the group

$$E_iH_i(-1)E_i = H_i(-1)$$
$$F_iH_i(-1)F_i = H_i(-1)$$

As a consequence of isotopy invariance, the situation can always be reduced to the case where a subword of the algebraic representative of the underlying braid is of the form $\sigma_i\sigma_i^{-1}$. We deal with the case where the orientations of the two concerned strands are positive, the other cases are similar. Diagrammatically the situation is described in the Figure 3.25.

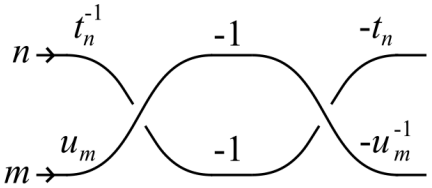

Figure 3.25: Local parameters for the second Reidemeister move.

The evaluation map gives

$$\begin{aligned} & H_i(t_n^{-1})H_{i+1}(u_m)F_iE_{i+1}H_i(-1)H_{i+1}(-1)F_iE_{i+1}H_i(-t_n)H_{i+1}(-u_m^{-1}) \\ = \; & H_i(t_n^{-1})H_{i+1}(u_m)F_iH_i(-1)F_iE_{i+1}H_{i+1}(-1)E_{i+1}H_i(-t_n)H_{i+1}(-u_m^{-1}) \\ = \; & H_i(t_n^{-1})H_{i+1}(u_m)H_i(-1)H_{i+1}(-1)H_i(-t_n)H_{i+1}(-u_m^{-1}) \\ = \; & H_i(1)H_{i+1}(1) \\ = \; & \mathrm{Id} \end{aligned}$$

This shows that

$$ev_{|S} \circ \psi^r(\sigma_i\sigma_i^{-1}, c) = ev_{|S} \circ \psi^r(1, c) \qquad \text{for all } i = 1, 2, \ldots, n-1$$

for the particular coloring and orientations considered. The other cases are similar, as is the demonstration of the equality

$$ev_{|S} \circ \psi^r(\sigma_i^{-1}\sigma_i,) = ev_{|S} \circ \psi^r(1, c) \qquad \text{for all } i = 1, 2, \ldots, n-1$$

The map ρ coincides with the generalized Burau representation

We have, at the moment of writing, no other demonstration that ρ coincides with the projectivized generalized Burau representation than a direct verification that the matrices coincide.

We believe that we could give a demonstration in the same spirit as the construction of section 3.1. That is, starting from a geometric braid, we can endow its exterior in a cylinder with a cellular structure, in the same way we did for link exteriors. It turns out that the bipartite graph encoding the 2-skeleton is equivalent to the one obtained from the Thurston diagrams we associated to braid diagrams. And the cluster variables are, up to sign, the monodromies of a local coefficients system induced by the abelianization morphism of the fundamental group of the braid exterior.

Remark – Applying the following rule, we obtain matrices of the same dimension as the usual Burau matrices. But we obtain only a projective representation.

$$\begin{aligned} \mathfrak{F}_{n-1} &\to \mathfrak{W}_{n-2} \\ \sigma_i &\mapsto s_{\overline{i-1}}s_i \\ \sigma_i^{-1} &\mapsto s_i s_{\overline{i-1}} \end{aligned}$$

Remark – We could also have done similar constructions but using the map $\sigma_i \mapsto s_i s_{\overline{i+1}}$. From the point of view of matrices, this construction is the transpose of the one we have presented.

3.2.3 Burau cluster submanifolds associated to oriented colored braids, the unreduced case

The construction of the preceding subsection had a topological motivation, in the sense that we transposed the construction of section 3.1 in the context of braids. But, from a

Lie theoretic point of view, there is a more natural candidate for the application which associates to an algebraic braid representative, a word in the braid semigroup. This is the map ψ_u defined below. This map and an appropriate construction of a submanifold will also give a representation of the colored oriented braid groupoid, in that case, a projective version of the generalized unreduced Burau representation for colored oriented braids. However we do not have, for the moment, a topological interpretation for the submanifold parameters.

In this subsection we construct the map ψ^u from the set of representatives of colored oriented braids on n strands to the set of pairs consisting of an A_{n-1} type cluster $\mathcal{X}$-manifold and a submanifold of it.

$$Br_n^c \xrightarrow{\psi^u} \{(\mathcal{X}_{A_{n-1}} - \text{manifold},\ \text{submanifold})\}$$

First, we define the ambient cluster $\mathcal{X}$-manifold : algebraically by assigning to an algebraic representative of the underlying braid, an element of the braid semigroup; and diagrammatically by associating Thurston diagrams to diagrammatic braid representatives. Then we give the rule of construction of the submanifolds.

Construction of the ambient manifold

Let β_c^r be a colored oriented braid representative on n strands and $\beta^r \in B_n$ the underlying braid representative. We associate to β^r an element of $\mathfrak{W}_{n-1}$ with the morphism of semigroups ψ defined below :

$$\begin{aligned} \psi_u : \mathfrak{F}_{n-1} &\to \mathfrak{W}_{n-1} \\ \sigma_i &\mapsto s_i s_{\bar{i}} \\ \sigma_i^{-1} &\mapsto s_{\bar{i}} s_i \end{aligned}$$

Recall from section 1.1 that to the element $\psi(\beta^r)$ of $\mathfrak{W}_{n-1}$ corresponds a seed, $\mathcal{X}_{\mathbf{J}(\psi_u(\beta^r))}$, of the A_{n-1} cluster $\mathcal{X}$-manifold associated to $p(\psi(\beta^r)) \in \mathcal{B}$. Diagrammatically the construction of the manifolds for the braid representatives semigroup generators translates in Figure 3.26 and Figure 3.27.

Construction of the submanifolds

In the unreduced case, cluster variables are associated to crossings of the braid and to regions of the braid diagram, that is, to the complementary faces in the plane of the underlying four-valent graph. The local rules for the construction of the cluster submanifolds corresponding to the unreduced Burau representation are given in Figure 3.28 and Figure 3.29 in the case where the strands are positively oriented.

Changing the orientation of a strand induces a change of variable of the form

$$t \mapsto -t^{-1}$$

where t is the variable assigned to the concerned strand.

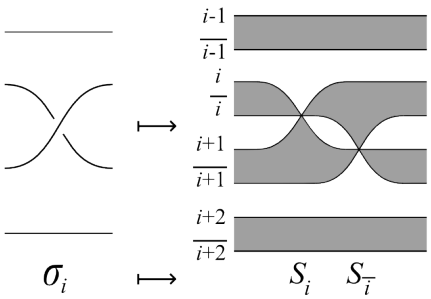

Figure 3.26: Diagrammatic rule for the construction of the ambient manifold associated to a positive braid generator in the unreduced case.

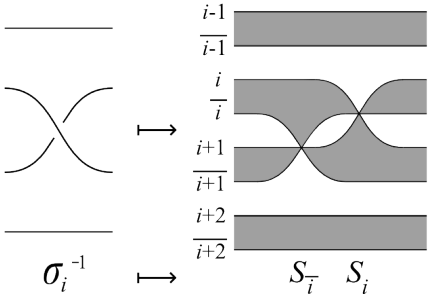

Figure 3.27: Diagrammatic rule for the construction of the ambient manifold associated to a negative braid generator in the unreduced case

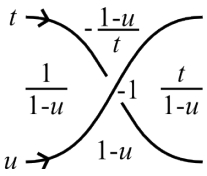

Figure 3.28: Submanifold parameters for the submanifold associated to a positive braid generator.

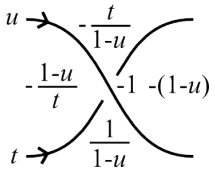

Figure 3.29: Submanifold parameters for the submanifold associated to a negative braid generator.

3.2.4 Demonstration of theorem 3.2

For the same arguments as in the beginning of the demonstration of theorem 3.1 in subsection 3.2.2, it suffices to show that

$$\begin{aligned}
ev_{|S} \circ \psi^u(\sigma_i\sigma_j, c) &= ev_{|S} \circ \psi^u(\sigma_j\sigma_i, c) && \text{for all } i,j = 1,2,\dots,n-1 \text{ with } |i-j| \geq 2\\
ev_{|S} \circ \psi^u(\sigma_i\sigma_{i+1}\sigma_i, c) &= ev_{|S} \circ \psi^u(\sigma_{i+1}\sigma_i\sigma_{i+1}, c) && \text{for all } i = 1,2,\dots,n-2\\
ev_{|S} \circ \psi^u(\sigma_i\sigma_i^{-1}, c) &= ev_{|S} \circ \psi^u(1, c) && \text{for all } i = 1,2,\dots,n-1\\
ev_{|S} \circ \psi^u(\sigma_i^{-1}\sigma_i,) &= ev_{|S} \circ \psi^u(1, c) && \text{for all } i = 1,2,\dots,n-1
\end{aligned}$$

And, as in the case of the map ψ^r we are in fact going to show that

$$\begin{aligned}
\psi^u(\sigma_i\sigma_j, c) &= \psi^u(\sigma_j\sigma_i, c) && \text{for all } i,j = 1,2,\dots,n-1 \text{ with } |i-j| \geq 2\\
\psi^u(\sigma_i\sigma_{i+1}\sigma_i, c) &= \psi^u(\sigma_{i+1}\sigma_i\sigma_{i+1}, c) && \text{for all } i = 1,\dots,n-2
\end{aligned}$$

That is, the ψ^u upgrades to a map from the positive colored oriented braids to the

set of pairs consisting of an A_{n-1} $\mathcal{X}$-manifold and a submanifold of it.

Invariance under commuting relations

Invariance under commuting relations, or diagrammatically, isotopy invariance, is a consequence of the first and second items of the theorem 1.1 in subsection 1.3.4. That is, the seeds we associate to braid representatives related by commuting relations are isomorphic. Let us consider i and j with $|i-j| \geq 2$. We have :

$$\psi_u(\sigma_i\sigma_j) = s_i s_{\bar{i}} s_j s_{\bar{j}}$$
$$\psi_u(\sigma_j\sigma_i) = s_j s_{\bar{j}} s_i s_{\bar{i}}$$

The corresponding words in the braid semigroup are related by the following sequence of relations which, according to theorem 1.1, induce isomorphisms of the corresponding seeds.

$$s_i s_{\bar{i}} s_j s_{\bar{j}} \to s_i s_j s_{\bar{i}} s_{\bar{j}} \to s_i s_j s_{\bar{j}} s_{\bar{i}} \to s_j s_i s_{\bar{j}} s_{\bar{i}} \to s_j s_{\bar{j}} s_i s_{\bar{i}}$$

This shows that, independently of the coloring function c, we have

$$\psi^r(\sigma_i\sigma_j, c) = \psi^r(\sigma_j\sigma_i, c) \text{ for all } i, j \ = 1, 2, \ldots, n-1 \text{ with } |i-j| \geq 2$$

And thus, invariance under commuting relations.

Invariance under the third Reidemeister move

We need to verify that :

$$\psi^u(\sigma_i\sigma_{i+1}\sigma_i, c) = \psi^u(\sigma_{i+1}\sigma_i\sigma_{i+1}, c)$$

We consider the case where $i > 1$, the three braided strands have a different color and are all oriented positively. The other cases are obtained by a change of variables. The situation is depicted in Figure 3.30 and Figure 3.31.

We have :

$$\psi_u(\sigma_i\sigma_{i+1}\sigma_i) = s_i s_{\bar{i}} s_{i+1} s_{\overline{i+1}} s_i s_{\bar{i}}$$
$$\psi_u(\sigma_{i+1}\sigma_i\sigma_{i+1}) = s_{i+1} s_{\overline{i+1}} s_i s_{\bar{i}} s_{i+1} s_{\overline{i+1}}$$

These two words are equal in the braid semigroup and, therefore, the associated seeds are two charts of the same cluster manifold. The two words are related by the following sequence, where braces indicate where the transformation occur. We precise next to the words the nature of the induced cluster transformation.

1. $s_i \underbrace{s_{\bar{i}} s_{i+1}} \underbrace{s_{\overline{i+1}} s_i} s_{\bar{i}}$ 2 isomorphisms

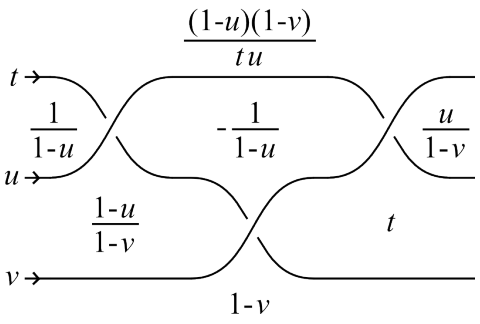

Figure 3.30: Oriented colored braid weighted diagram whose underlying algebraic braid representative is $\sigma_i\sigma_{i+1}\sigma_i$

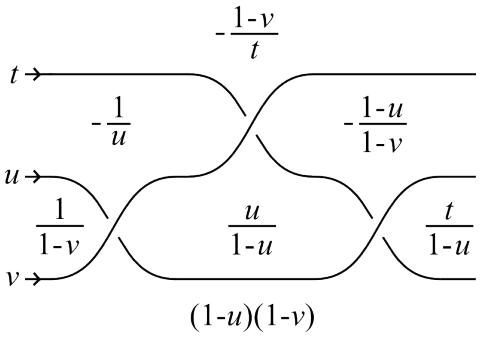

Figure 3.31: Oriented colored braid weighted diagram whose underlying algebraic braid representative is $\sigma_{i+1}\sigma_i\sigma_{i+1}$

2. $s_i s_{i+1} \underbrace{s_{\bar{i}} s_i}\ s_{\overline{i+1}} s_{\bar{i}}$ 1 mutation

3. $\underbrace{s_i s_{i+1} s_i}\ s_{\bar{i}} s_{\overline{i+1}} s_{\bar{i}}$ 1 mutation

4. $s_{i+1} s_i s_{i+1} \underbrace{s_{\bar{i}} s_{\overline{i+1}} s_{\bar{i}}}$ 1 mutation

5. $s_{i+1} s_i \underbrace{s_{i+1} s_{\overline{i+1}}}\ s_{\bar{i}} s_{\overline{i+1}}$ 1 mutation

6. $s_{i+1} \underbrace{s_i s_{\overline{i+1}}} \underbrace{s_{i+1} s_{\bar{i}}}\ s_{\overline{i+1}}$ 2 isomorphisms

7. $s_{i+1} s_{\overline{i+1}} s_i s_{\bar{i}} s_{i+1} s_{\overline{i+1}}$

These transformations and the transformations of the submanifold parameters are represented in the following Thurston diagrams.

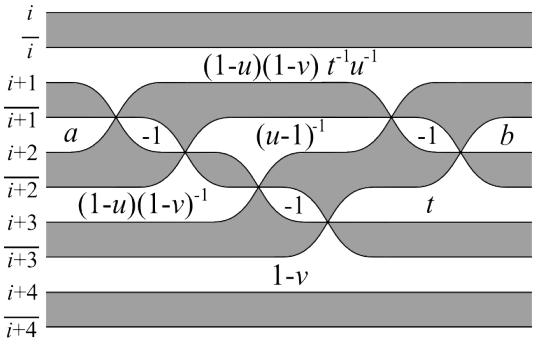

Figure 3.32: Thurston diagram description of the seed corresponding to $s_i s_{\bar{i}} s_{i+1} s_{\overline{i+1}} s_i s_{\bar{i}}$, and submanifold parameters where $a = \frac{1}{1-u}$ and $b = \frac{u}{1-v}$.

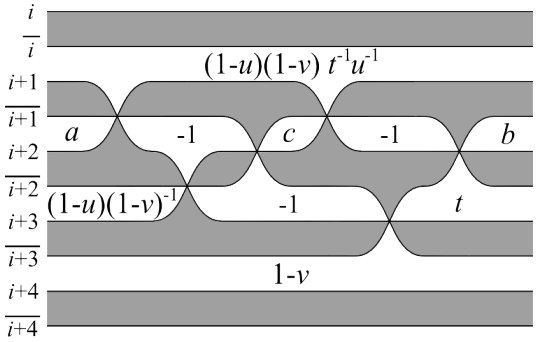

Figure 3.33: Thurston diagram description of the seed corresponding to $s_i s_{i+1} s_{\bar{i}} s_i s_{\overline{i+1}} s_{\bar{i}}$, and submanifold parameters where $a = \frac{1}{1-u}$, $b = \frac{u}{1-v}$ and $c = \frac{-1}{1-u}$.

This diagram is obtained from the one in Figure 3.32 by a gray move and an isotopy.

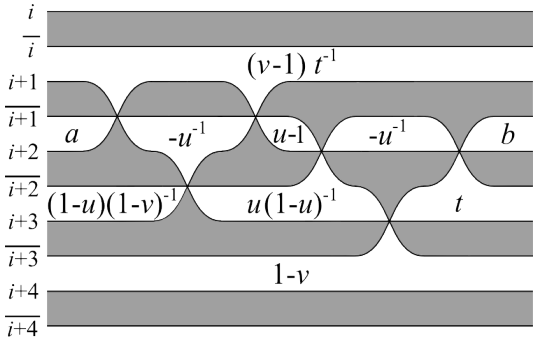

Figure 3.34: Thurston diagram description of the seed corresponding to $s_i s_{i+1} s_i s_{\bar{i}} s_{\overline{i+1}} s_{\bar{i}}$, and submanifold parameters where $a = \frac{1}{1-u}$ and $b = \frac{u}{1-v}$.

This diagram is obtained from the one in Figure 3.33 by a white move in the face with the variable c.

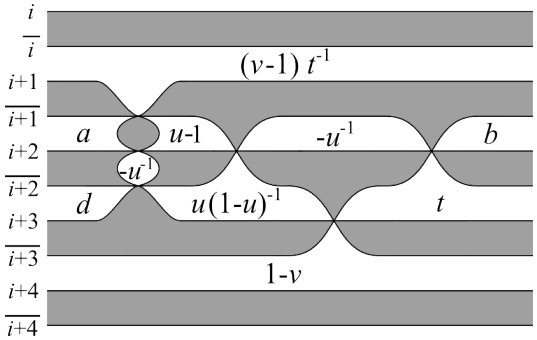

Figure 3.35: Thurston diagram obtained from the one in Figure 3.34 by a gray move, and submanifold parameters where $a = \frac{1}{1-u}$, $b = \frac{u}{1-v}$ and $d = \frac{1-u}{1-v}$.

Note that this diagram does not correspond to any word in $\mathfrak{W}$.

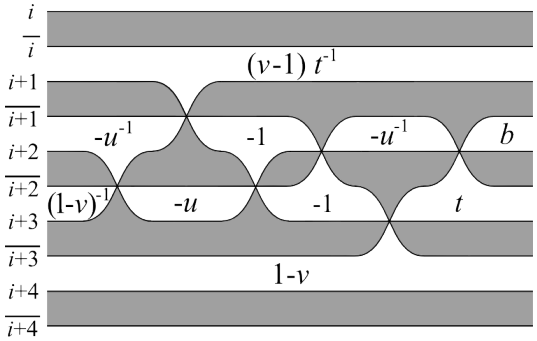

Figure 3.36: Thurston diagram description of the seed corresponding to $s_{i+1} s_i s_{i+1} s_{\bar{i}} s_{\overline{i+1}} s_{\bar{i}}$, and submanifold parameters where $b = \frac{u}{1-v}$.

This diagram is obtained from the one in Figure 3.35 by a gray move.

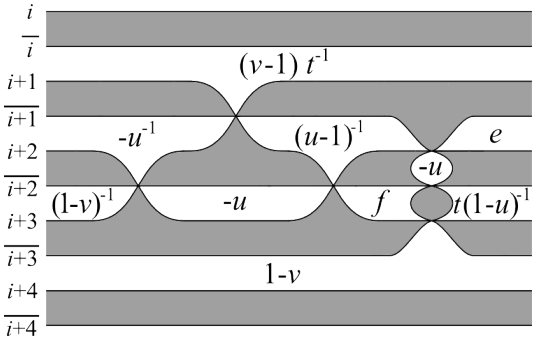

Figure 3.37: Thurston diagram description of the seed corresponding to $s_{\bar{i}}s_{i+1}s_{\overline{i+1}}s_{i+2}s_{\bar{i}}s_{i+1}$, and submanifold parameters where $e = \frac{u-1}{1-v}$ and $f = \frac{1-u}{u}$.

This diagram is obtained from the one in Figure 3.36 by a white move in the rightmost face with the variable $-u$.

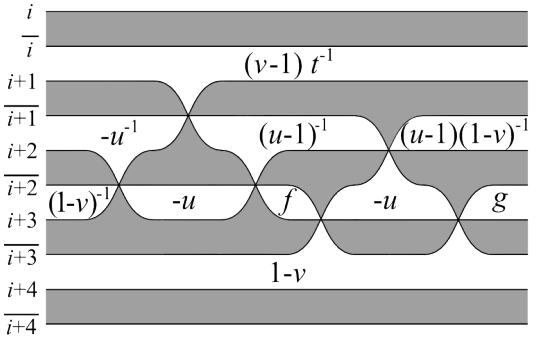

Figure 3.38: Thurston diagram description of the seed corresponding to $s_{i+1}s_is_{i+1}s_{\overline{i+1}}s_{\bar{i}}s_{\overline{i+1}}$, and submanifold parameters where $f = \frac{1-u}{u}$ and $g = \frac{t}{1-u}$.

This diagram is obtained from the one in Figure 3.37 by a gray move.

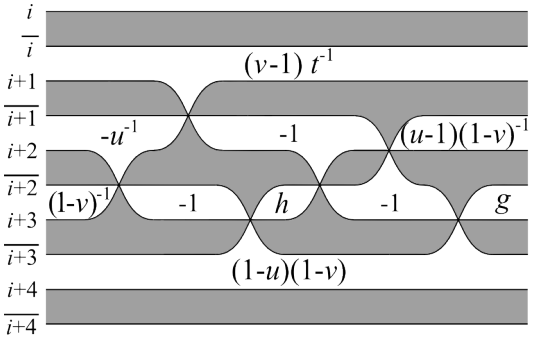

Figure 3.39: Thurston diagram description of the seed corresponding to $s_{i+1}s_is_{\overline{i+1}}s_{i+1}s_{\bar{i}}s_{\overline{i+1}}$, and submanifold parameters where $g = \frac{t}{1-u}$ and $h = \frac{1-u}{u}$.

This diagram is obtained from the one in Figure 3.38 by a white move in the face with the variable f.

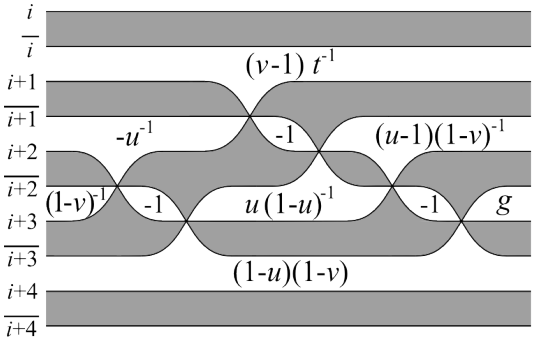

Figure 3.40: Thurston diagram description of the seed corresponding to $s_{i+1}s_{\overline{i+1}}s_is_{\bar{i}}s_{i+1}s_{\overline{i+1}}$, and submanifold parameters where $g = \frac{t}{1-u}$.

This diagram is obtained from the one in Figure 3.39 by an isotopy and a gray move.

The results of the evaluation map on the corresponding seed tori are given below where we have set $i = 2$ to simplify notations. The braces indicate where mutations occur. Item k is the result of the evaluation map on the submanifold associated to the

colored braid representative in Figure 3.30 in the seed corresponding to the word in item k of the list beginning page 46.

1. $H_1(\frac{(1-u)(1-v)}{tu})H_2(\frac{1}{1-u})H_3(\frac{1-u}{1-v})H_4(1-v)E_2H(-1)F_2H_2(-\frac{1}{1-u})E_3H_3(-1)F_3\dots$
   $\dots E_2H_2(-1)F_2H_2(\frac{u}{1-v})H_3(t)$

2. $H_1(\frac{(1-u)(1-v)}{tu})H_2(\frac{1}{1-u})H_3(\frac{1-u}{1-v})H_4(1-v)E_2H_2(-1)E_3\underbrace{F_2H_2(-\frac{1}{1-u})E_2}H_3(-1)\dots$
   $\dots F_3H_2(-1)F_2H_2(\frac{u}{1-v})H_3(t)$

3. $H_1(-\frac{1-v}{t})H_2(\frac{1}{1-u})H_3(\frac{1-u}{1-v})H_4(1-v)\underbrace{E_2H_2(-\frac{1}{u})E_3E_2}H_3(\frac{u}{1-u})H_2(u-1)F_2F_3\dots$
   $\dots H_2(-\frac{1}{u})F_2H_2(\frac{u}{1-v})H_3(t)$

4. $H_1(-\frac{1-v}{t})H_2(-\frac{1}{u})H_3(\frac{1}{1-v})H_4(1-v)E_3H_3(-u)E_2E_3H_2(-1)H_3(-1)\dots$
   $\dots\underbrace{F_2F_3H_2(-\frac{1}{u})F_2}H_2(\frac{u}{1-v})H_3(t)$

5. $H_1(-\frac{1-v}{t})H_2(-\frac{1}{u})H_3(\frac{1}{1-v})H_4(1-v)E_3H_3(-u)E_2H_2(-\frac{1}{1-u})\dots$
   $\dots\underbrace{E_3H_3(\frac{1-u}{u})F_3}H_3(-u)F_2F_3H_2(\frac{u-1}{1-v})H_3(\frac{t}{1-u})$

6. $H_1(-\frac{1-v}{t})H_2(-\frac{1}{u})H_3(\frac{1}{1-v})H_4((1-u)(1-v))E_3H_3(-1)E_2H_2(-1)F_3H_3(\frac{u}{1-u})\dots$
   $\dots E_3H_3(-1)F_2F_3H_3(-\frac{1-u}{1-v})H_3(\frac{t}{1-u})$

7. $H_1(-\frac{1-v}{t})H_2(-\frac{1}{u})H_3(\frac{1}{1-v})H_4((1-u)(1-v))E_3H_3(-1)F_3E_2H_2(-1)F_2\dots$
   $\dots H_3(\frac{u}{1-u})E_3H_3(-1)F_3H_2(-\frac{1-u}{1-v})H_3(\frac{t}{1-u})$

Invariance under the second Reidemeister move

Invariance under the second Reidemeister move is a consequence of the following relations between the generators of the group

$$E_iH_i(-1)E_i = H_i(-1)$$
$$F_iH_i(-1)F_i = H_i(-1)$$

As a consequence of isotopy invariance, the situation can always be reduced to the case where a subword of the algebraic representative of the underlying braid is of the form $\sigma_i\sigma_i^{-1}$. We deal with the case where $2 \leq i \leq n-2$ and the orientations of the two concerned strands are positive, the other cases are similar. Diagrammatically the situation is described in the Figure 3.41.

The evaluation map gives

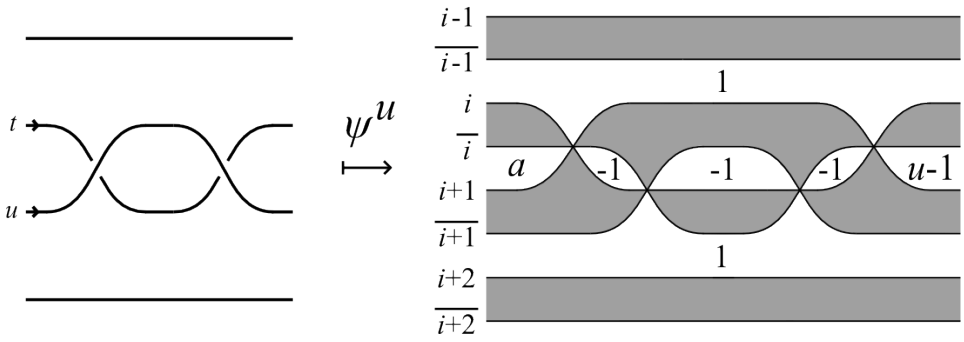

Figure 3.41: Thurston diagram description of $\psi^u(\sigma_i\sigma_i^{-1}, c)$ where $a = \frac{1}{1-u}$.

$$\begin{aligned} & H_{i-1}(1)H_i(\tfrac{1}{1-u})H_{i+1}(1)E_iH_i(-1)F_iH_i(-1)F_iH_i(-1)E_iH_i(u-1) \\ = \;& H_i(\tfrac{1}{1-u})E_iH_i(-1)E_iH_i(u-1) \\ = \;& H_i(\tfrac{1}{1-u})H_i(-1)H_i(u-1) \\ = \;& \mathrm{Id} \end{aligned}$$

This shows that

$$ev_{|S} \circ \psi^r(\sigma_i\sigma_i^{-1}, c) = ev_{|S} \circ \psi^r(1, c)$$

for $i = 2, \ldots, n-2$ and for the particular coloring and orientation considered. The other cases are similar, as is the demonstration of the equality

$$ev_{|S} \circ \psi^r(\sigma_i^{-1}\sigma_i,) = ev_{|S} \circ \psi^r(1, c) \qquad \text{for all } i = 1, 2, \ldots, n-1$$

3.3 Burau cluster submanifolds associated to annular braids

The constructions of the preceding section extend almost straightforwardly from A_n to $\widehat{A}_n$. Colored oriented braids are replaced by cylindrical colored oriented braids, cluster $\mathcal{X}$-manifolds of type A_n by those of type $\widehat{A}_n$. The major difference comes from the additional generator τ of the annular braid group, but it is handled by the coextension generator l of the Weyl group. A priori, the evaluation map gives infinite matrices, but it turns out, as the product of the parameters defining our submanifolds is equal to one, that we obtain finite matrices.

We construct the analogues in the affine case of the maps ψ^r and ψ^u of the section 3.2

$$\widehat{B}r_n^c \xrightarrow{\widehat{\psi}^r} \{(\mathcal{X}_{\widehat{A}_{n-1}} - \text{manifold},\ \text{submanifold})\} \tag{3.3}$$

$$\widehat{B}r_n^c \xrightarrow{\widehat{\psi}^u} \{(\mathcal{X}_{\widehat{A}_{n-1}} - \text{manifold},\ \text{submanifold})\} \tag{3.4}$$

And we prove the corresponding theorems

In subsection 3.3.1 we construct the map $\widehat{\psi}^r$ and prove the following theorem.

Theorem 3.3 *For $n \geq 3$, let $\widehat{\rho} : \widehat{B}_n^c \to PGL_n(\mathbb{Q}(t_1, u_1, \ldots, t_n, u_n))$ be the composition of the map r, which assigns an arbitrary representative to colored oriented annular braid, with $\widehat{\psi}^r$ and the evaluation map restricted to the second factor :*

$$\widehat{\rho} : \widehat{B}_n^c \xrightarrow{r} \widehat{B}r_n^c \xrightarrow{\widehat{\psi}^r} \{(M_{\widehat{A}_{n-1}}, S)\} \xrightarrow{ev_{|S}} PGL_n(\mathbb{Q}(t_1, u_1, \ldots, t_n, u_n))$$

The map $\widehat{\rho}$ is a projective representation of the colored oriented annular braids on n strands groupoid, which coincides with the projectivization of the generalized reduced Burau representation.

In subsection 3.3.3 we construct the map $\widehat{\psi}^u$ and prove the corresponding theorem.

Theorem 3.4 *For $n \geq 3$, let $\widehat{\rho}_u : \widehat{B}_n^c \to PGL_n(\mathbb{Q}(t_1, \ldots, t_n))$ be the composition of the map r, which assigns an arbitrary representative to colored oriented braid, with $\widehat{\psi}^u$ and the evaluation map restricted to the second factor :*

$$\widehat{\rho}_u : \widehat{B}_n^c \xrightarrow{r} \widehat{B}r_n^c \xrightarrow{\widehat{\psi}^u} \{(M_{\widehat{A}_{n-1}}, S)\} \xrightarrow{ev_{|S}} PGL_n(\mathbb{Q}(t_1, \ldots, t_n))$$

The map $\widehat{\rho}_u$ is a projective representation of the colored oriented annular braidson n strands groupoid, which coincides with the projectivization of the generalized unreduced Burau representation.

3.3.1 Burau cluster submanifolds associated to oriented colored annular braids, the reduced case

Construction of the ambient manifold

Let $\widehat{\beta}_c^r$ be a colored oriented annular braid on n strands representative and $\widehat{\beta}^r \in \widehat{B}_n$ the underlying annular braid representative. We associate to $\widehat{\beta}^r$ an element of $\widehat{\mathfrak{W}}_{n-1}$ with the morphism of semigroups $\widehat{\psi}$ defined below.

$$\begin{aligned} \psi : \mathfrak{F}_{2n+1} &\to \widehat{\mathfrak{W}}_{n-1} \\ \sigma_i &\mapsto s_{\bar{i}} s_{i+1} \\ \sigma_i^{-1} &\mapsto s_{i+1} s_{\bar{i}} \\ \tau &\mapsto l \end{aligned}$$

where the indices are to be understood modulo n.

Construction of the submanifold

The parameters defining the cluster submanifolds are defined in the exact same way as in the case of the classical colored oriented braids. The parameters correspond to half arcs of the annular braid diagram and are determined by the same rule as in subsection 3.2.1. We recall for convenience the rule in Figure 3.42 and Figure 3.43.

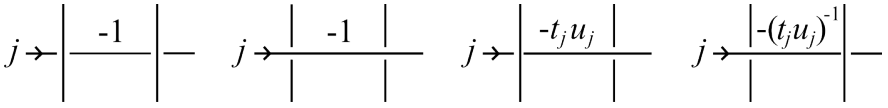

Figure 3.42: Submanifold parameters for internal half arcs.

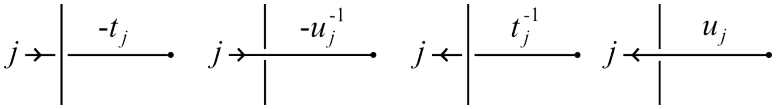

Figure 3.43: Submanifold parameters for terminal half arcs.

3.3.2 Demonstration of theorem 3.3

All the arguments of the demonstration of theorem 3.1 are valid in the affine case. It remains to show that :

$$ev_{|S} \circ \widehat{\psi}^r(\sigma_i\tau, c) = ev_{|S} \circ \widehat{\psi}^r(\tau\sigma_{i+1}, c)$$

This equality is a consequence of the relations :

$$E_i\Lambda = \Lambda E_{i+1}, \quad F_i\Lambda = \Lambda F_{i+1}, \quad H_i(x)\Lambda = \Lambda H_{i+1}(x), \quad i \in \mathbb{Z}/N\mathbb{Z}$$

We consider the case where all the strands are positively oriented and where the i-th strand is colored with i and the $i+1$-th with $i+1$.

We have :

$$\begin{aligned} ev_{|S} \circ \widehat{\psi}^r(\sigma_i\tau, c) &= H_i(t_i^{-1})H_{i+1}(u_{i+1})F_iE_{i+1}H_i(-u_{i+1}^{-1})H_{i+1}(-t_i)\Lambda \\ &= \Lambda H_{i+1}(t_i^{-1})H_{i+2}(u_{i+1})F_{i+1}E_{i+2}H_{i+1}(-u_{i+1}^{-1})H_{i+2}(-t_i) \\ &= ev_{|S} \circ \widehat{\psi}^r(\tau\sigma_{i+1}, c) \end{aligned}$$

3.3.3 Burau cluster submanifolds associated to oriented colored annular braids, the unreduced case

Construction of the ambient manifold

Let $\widehat{\beta}_c^r$ be a colored oriented annular braid on n strands representative and $\widehat{\beta}^r \in \widehat{B}_n$ the underlying annular braid representative. We associate to $\widehat{\beta}^r$ an element of $\widehat{\mathfrak{W}}_{n-1}$ with

the morphism of semigroups $\widehat{\psi}_u$ defined below.

$$\begin{aligned}\psi_u : \mathfrak{F}_{2n+1} &\to \widehat{\mathfrak{W}}_{n-1}\\ \sigma_i &\mapsto s_i s_{\bar{i}}\\ \sigma_i^{-1} &\mapsto s_{\bar{i}} s_i\\ \tau &\mapsto l\end{aligned}$$

where the indices are to be understood modulo n.

Construction of the submanifold

As in the case of classical braids, cluster variables correspond to the faces of the braid diagram and we define our submanifolds with the same parameters as in the classical case. The local rules for the construction of the cluster submanifolds is recalled in the Figure 3.44 and Figure 3.45 in the case where the strands are positively oriented.

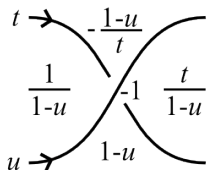

Figure 3.44: Submanifold parameters for the submanifold associated to a positive braid generator.

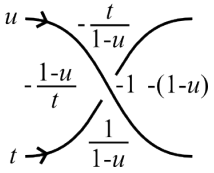

Figure 3.45: Submanifold parameters for the submanifold associated to a negative braid generator.

Changing the orientation of a strand induces a change of variable of the form

$$t \mapsto -t^{-1}$$

where t is the variable assigned to the concerned strand.

3.3.4 Demonstration of theorem 3.4

Again, all the arguments of the demonstration of theorem 3.2 are valid in the affine case. It remains to show that :

$$ev_{|S} \circ \widehat{\psi}^u(\sigma_i\tau, c) = ev_{|S} \circ \widehat{\psi}^u(\tau\sigma_{i+1}, c)$$

This equality is a consequence of the relations :

$$E_i\Lambda = \Lambda E_{i+1}, \quad F_i\Lambda = \Lambda F_{i+1}, \quad H_i(x)\Lambda = \Lambda H_{i+1}(x), \quad i \in \mathbb{Z}/N\mathbb{Z}$$

We consider the case where all the strands are positively oriented and where the i-th strand is assigned with the variable t and the $i+1$-th with u.

We have :

$$\begin{aligned} ev_{|S} \circ \widehat{\psi}^u(\sigma_i \tau, c) &= H_{i-1}(\frac{u-1}{t}) H_i(\frac{1}{1-u}) H_{i+1}(1-u) E_i H_i(-1) F_i H_i(\frac{t}{1-u}) \Lambda \\ &= \Lambda H_i(\frac{u-1}{t}) H_{i+1}(\frac{1}{1-u}) H_{i+2}(1-u) E_{i+1} H_{i+1}(-1) F_{i+1} H_{i+1}(\frac{t}{1-u}) \\ &= ev_{|S} \circ \widehat{\psi}^u(\tau \sigma_{i+1}, c) \end{aligned}$$

Bibliography

[All02] Daniel Allcock. Braid pictures for artin groups. Transactions of the American Mathematical Society, 354(9):3455–3474, 2002.

[Bur35] Werner Burau. Über zopfgruppen und gleichsinnig verdrillte verkettungen. In Abhandlungen aus dem Mathematischen Seminar der Universität Hamburg, volume 11, pages 179–186. Springer, 1935.

[CDR14] Moshe Cohen, Oliver T Dasbach, and Heather M Russell. A twisted dimer model for knots. Fundamenta mathematicae, 225(1):57–74, 2014.

[Coh73] Marshall M Cohen. A course in simple-homotopy theory. 1973.

[FG06a] Vladimir Fock and Alexander Goncharov. Moduli spaces of local systems and higher teichmüller theory. Publications Mathématiques de l'IHÉS, 103:1–211, 2006.

[FG06b] Vladimir V Fock and Alexander B Goncharov. Cluster χ-varieties, amalgamation, and poisson—lie groups. In Algebraic geometry and number theory, pages 27–68. Springer, 2006.

[FG07] Vladimir V Fock and Alexander B Goncharov. Dual teichmüller and lamination spaces. Handbook of Teichmüller theory, 1(11):647–684, 2007.

[FM14] VV Fock and A Marshakov. Integrable systems, cluster variables, and dimers. arXiv preprint arXiv:1401.1606, 2014.

[FZ02] Sergey Fomin and Andrei Zelevinsky. Cluster algebras i: foundations. Journal of the American Mathematical Society, 15(2):497–529, 2002.

[GK11] Alexander B Goncharov and Richard Kenyon. Dimers and cluster integrable systems. arXiv preprint arXiv:1107.5588, 2011.

[GSV03] Michael Gekhtman, Michael Zalmanovich Shapiro, and Alek D Vainshtein. Cluster algebras and poisson geometry. Moscow Mathematical Journal, 3(3):899–934, 2003.

[GTW17] Agnès Gadbled, Anne-Laure Thiel, and Emmanuel Wagner. Categorical action of the extended braid group of affine type a. Communications in Contemporary Mathematics, 19(03):1650024, 2017.

[Jon85] Vaughan FR Jones. A polynomial invariant for knots via von neumann algebras. Bulletin of the American Mathematical Society, 12(1):103–111, 1985.

[Kau06] Louis H Kauffman. Formal knot theory. Courier Corporation, 2006.

[KIP02] Richard P Kent IV and David Peifer. A geometric and algebraic description of annular braid groups. International Journal of Algebra and Computation, 12(01n02):85–97, 2002.

[KNS11] Atsuo Kuniba, Tomoki Nakanishi, and Junji Suzuki. T-systems and y-systems in integrable systems. Journal of Physics A: Mathematical and Theoretical, 44(10):103001, 2011.

[KT08] Christian Kassel and Vladimir Turaev. Braid groups, volume 247. Springer Science & Business Media, 2008.

[SW01] Daniel S Silver and Susan G Williams. A generalized burau representation for string links. Pacific Journal of Mathematics, 197(1):241–255, 2001.

[Thu04] Dylan P Thurston. From dominoes to hexagons. arXiv preprint math/0405482, 2004.

[Tur86] Vladimir G Turaev. Reidemeister torsion in knot theory. Russian Mathematical Surveys, 41(1):119–182, 1986.

[Tur12] Vladimir Turaev. Introduction to combinatorial torsions. Birkhäuser, 2012.

Nicolas PASTANT

Théorie des nœuds et variétés amassées

Résumé

Dans cette thèse nous établissons des liens entre la théorie des nœuds et la théorie des variétés amassées. Nous réinterprétons le modèle de dimères pour le polynôme d'Alexander d'un nœud de Cohen, Dasbach et Russel dans le contexte des variétés amassées. Nous étendons le modèle à la torsion de Milnor de l'extérieur d'un entrelacs. Nous construisons une application qui associe à un représentant de tresse colorée et orientée, une paire consistant en une variété amassée modelée sur le diagramme Dynkin de type A et une sous-variété de cette dernière. Les variétés modelées sur le diagramme de Dynkin de type A, construites par Fock et Goncharov, sont munies d'une application d'évaluation. La composition de notre l'application avec l'application d'évaluation restreinte à la sous-variété donne une généralisation de la représentation de Burau réduite du groupoïde des tresses colorées et orientées. Nous donnons une construction similaire pour la représentation de Burau non réduite du groupoïde des tresses colorées et orientées. Nous adaptons les deux constructions précédentes pour les tresses cylindriques colorées orientées. Dans ce cas, les variétés amassées associées sont modelées sur le diagramme de Dynkin de type A affine.

Mots-clés : Théorie des nœuds, groupes de tresses, variétés amassées.

Résumé en anglais

In this thesis we establish connections between knot theory and the theory of cluster varieties. We reinterpret the dimer model for the Alexander polynomial of a knot of Cohen, Dasbach and Russel in the context of cluster varieties. We extend the model to the Milnor torsion of a link exterior. We construct an application which associates with a representative of a colored and oriented braid, a pair consisting of a cluster variety modeled on the type A Dynkin diagram and a sub-variety of the latter. The varieties modeled on the type A Dynkin diagram, constructed by Fock and Goncharov, are equipped with an evaluation map. The composition of our application with the evaluation map restricted to the sub-variety gives a generalization of the reduced Burau representation of the groupoid of colored and oriented braids. We give a similar construction for the unreduced Burau representation of the groupoid of colored and oriented braids. We adapt the two previous constructions for the colored oriented cylindrical braids. In this case, the associated cluster varieties are modeled on the affine type A Dynkin diagram.

Keywords : Knot theory, braid groups, cluster varieties.